The Effect of Human Immunodeficiency Virus Type-1 Coreceptor Preference on Entry and Tropism Specific Phenotypes

By

Melissa Zarr

A dissertation submitted to Johns Hopkins University in conformity with the requirements for the degree of Doctor of Philosophy

Baltimore MD

June 2014

Abstract

During HIV type 1 (HIV-1) entry, trimers of viral gp120 proteins attach to CD4 molecules and to CCR5 or CXCR4 coreceptors on the target cell. A virus is defined as R5 tropic if it uses CCR5 coreceptors and X4 tropic if it uses CXCR4. In addition to the difference in coreceptor usage, R5 and X4 tropic viruses display other phenotypic differences. R5 virus dominates in early infection even when recipients are co-infected with both viral tropisms. As the disease progresses, the virus evolves and a tropism switch from R5 to X4 occurs in approximately 50% of patients. This study aims to more fully elucidate the mechanisms underlying the phenotypic differences between X4 and R5 virus.

The stoichiometric parameters associated with HIV-1 target cell entry remain unclear and may differ depending on coreceptor usage. Important unanswered questions include: how many viral envelope trimers (or spikes) must attach to CD4 molecules, how many must bind coreceptors, and how many functional gp120 subunits per envelope trimer are required for entry? To answer these questions we performed single round infectivity assays with chimeric viruses. Theoretical relative infectivity curves were generated using mathematical models and compared to the experimental curves. Using this methodology we determined that HIV-1 entry requires only a small number (one or two) of functional envelope spikes. Our data indicate that an individual virion has between one and three envelope spikes on its surface that are both functional and able to simultaneously contact a target cell. In addition, our analysis shows that trimeric envelope spikes may function with fewer than three active gp120 subunits. However, our

analysis of the entry mechanism indicates that there is no major difference in the stoichiometric requirements for CCR5 versus CXCR4-mediated HIV-1 entry into host cells.

To investigate whether factors outside of viral entry machinery differentially affect the fitness of R5 and X4 tropic viruses, we used *in vitro* techniques to assay infection rates, target cell availability, viral burst size, and the potential negative pressure of the cytotoxic lymphocyte (CTL) response. Our study indicates that R5 virus has a kinetic advantage over X4 virus replication. Our results show that neither CTL suppression nor burst size correlates to tropism and thus is unlikely to play a role in early R5 viral dominance. Contrary to what is seen in newly infected patients, we saw consistently higher rates of infection with X4 virus. Viral growth modeling indicates that target cell availability in our *in vitro* system is responsible for this apparent X4 replication advantage. Infection rate constants for X4 and R5 virus, which are influenced by infection rate, burst size, and target cell availability, indicate that R5 virus has a more than two fold replication advantage over some of the X4 viral isolates. If target cell availability during early infection does not overwhelmingly favor X4 growth, then this kinetic difference could explain R5's initial dominance.

Overall, our data supports the hypothesis that credits replication rate and target cell availability for dominance of R5 tropic virus and for tropism switching respectively. We conclude that R5 virus more efficiently causes productive infection in its target cells and this gives it a replication advantage until those target cells are depleted. We conclusively show that initial advantage of R5 virus does not come from the entry machinery, from the viral burst size, or from CTL suppression of X4 infected cells.

Thesis Advisor: Robert F Siliciano M.D., Ph.D.

Thesis Reader: Craig Hendrix M.D., PhD.

Acknowledgements

Without my parents, I would not be the person I am today. I can blame nearly all of who I am on them; they are responsible for both nature and nurture. Over all of the years, without fail, their efforts to provide for, support, and encourage me go well above and beyond the standard parental obligation. They have always done absolutely everything in their power to provide me with the best opportunities and I could not be more grateful. I remember the long nights spent working on homework with me. I remember the dance lessons, the school trips, and the summer camps. I remember the years of support that enabled me to attend my dream college. I grew up feeling like I was the most loved and valued child in the world and that feeling has never left. Thank you for all of your time, effort and sacrifices; thank you for always encouraging me to be me. This PhD is as much yours as it is mine.

I am also infinitely grateful to my PI, Dr. Bob Siliciano. The Siliciano Laboratory environment is unique and it is wonderful. Here we have any support that we ask for and infinite freedom. If Bob had not decided to take a chance on me and welcome a third year graduate student into his lab I would not have completed my PhD. Now I am leaving Hopkins with not only a degree, but also with invaluable research experience.

Table of Contents

List of Tables and Figures

Chapter 1: Stoichiometric Parameters of HIV-1 Entry

Chapter 2: Investigating Possible Causes for R5 Tropism Dominance in Early Infection and Tropism Switching in Advanced Disease

Introduction

AIDS was first recognized as a disease in 1981. The causative agent of the disease is Human Immunodeficiency Virus (HIV-1), an RNA virus that infects and kills human immune cells. Antiretroviral drugs are now able to efficiently control HIV-1 replication and prevent the immune depletion that leads to AIDS but our understanding of the disease, and our control over it, remains incomplete. UNAIDS estimated that were 35.3 million people living with HIV and 2.3 million new HIV infections globally in 2012 [1].

The virus life cycle has several distinct phases. The first is viral entry into the target cell. This is followed by reverse transcription of its RNA. In the third phase the new viral DNA integrates into the host's genome where it waits for the host cell's machinery to produce the encoded viral proteins. The final phases are the assembly, the budding/release, and the maturation of the virus particle. This entire process, on average, takes 1.2 days [2].

The process by which an HIV-1 virion enters a human cell is complex and is still not entirely understood. Some studies have used electron microscopy to directly view various stages of entry and others have used biochemical techniques and modeling to quantitatively analyze the process. While some aspects of HIV-1 entry remain unclear, such as the exact number of binding events involved; others, such as the viral entry machinery and the basic order of events, have been well defined [3]. During viral development, envelope glycoproteins (Env) are produced and assembled into trimers (commonly called spikes) that protrude from the surface of the virion [4-8]. Each trimer

consists of three sets of noncovalently associated subunits, gp120 and gp41. Thus, spikes are homo-trimers composed of three hetero-dimers [9,10].

The first step in the entry process is viral attachment; here the virus's gp120 subunits bind to CD4 molecules on the surface of a host cell [11-15]. This binding induces a conformational change within the entry spike that activates the gp120s for coreceptor binding [16-24]. In the next step, the activated gp120 binds either the host cells CCR5 or CXCR4 chemokine receptors, which both function as coreceptors for HIV-1 [25-27]. This coreceptor binding causes the gp41 subunits to insert into the host cell membrane which initiates the fusion of the viral and cellular membranes.

The entry step of the HIV-1 life cycle is particularly significant to those investigating the difference between the HIV-1 tropisms. HIV-1 is divided into two varieties, called tropisms, based on the molecules it uses to enter a target cell. Current nomenclature classifies an HIV-1 isolate as R5 tropic if it uses the CCR5 co-receptor to enter a host cell, X4 tropic if it uses the CXCR4 coreceptor, and dual tropic (X4R5) if it can utilize either coreceptor for entry [28].

While there is no single DNA sequence that determines tropism, sequence analysis algorithms can be used to predict tropism with accuracies reaching 80-90% [29]. Coreceptor usage is primarily determined by the second and third variable loops (V2 and V3) of the gp120 subunit [30-33] and positively-charged amino acids at positions 11 and 25 within V3 are strongly associated with X4 tropism [34, 35]. However, while the genotypic differences certainly cause the phenotypic differences, the tropism

classification of a virus is a phenotypic observation and functional assays provide the most reliable assessment of coreceptor usage.

While similar in sequence, R5 and X4 viruses behave differently *in vivo* and the phenotypic differences extend beyond the coreceptor preferences that define them. In the acute phase of infection, R5 viruses usually predominate [36-42]. Even if the source patient has both R5 and X4 tropic viruses, R5 is normally the only viral variant detectable in the recipient [34-37]. This is widely documented and most commonly attributed to the bottle nose effect that mucosal membranes have on the incoming virus population. However, R5 selective transmission has been documented not only in intravaginal transmission cases but also in intravenous transmissions, in both Simian Immunodeficiency Virus (SIV) lab experiments and human needle stick case studies [43-45].

The second phenotypic difference between the two tropisms emerges predominantly in advanced stages of the disease. In what appears to be a natural result of disease progression, approximately 50% of HIV-1-infected patients experience a tropism switch where X4 virus emerges and then takes over, out competing the R5 virus. Much like the R5 tropic dominance in early infection, the reason why X4 virus often emerges and dominates in advanced stages of the disease remains a mystery. Interestingly, the emerging X4 virus most commonly is not an archived virus that surfaces from a latent reservoir. Instead, each patient's virus evolves and transitions through a dual tropic state to become X4 tropic [46]. Tropism switching is of particular interest clinically because the transition correlates with increased morbidity and mortality [47, 48]. Yet, while the effect a tropism switch has on a patient's overall immune system is clear, Sodroski, *et al*.,

show that the cytotoxic effects of R5 and X4 viruses on individual cells are the same [49].

The reduced transmissibility of X4 virus and its correlation with disease progression suggest that there are fundamental, biological differences between X4 and R5 tropic viruses. The most obvious difference is the one that defines tropism, coreceptor usage during the entry process. But the coreceptors themselves are merely tools that the virus uses to gain entry into a cell. Thus, more information is needed to explain the phenotypic differences between the tropisms.

Closely examining the entry mechanism may help solve some of the mystery surrounding phenotypic tropism differences. The stoichiometry of binding, for both CD4 and the coreceptors CXCR4 and CCR5, is still under debate [50]. In chemistry, stoichiometry refers to the relative quantities of reactants and products; in HIV-1 entry it refers to the number of spikes, or gp120 subunits with-in a spike that must bind a corresponding number of receptors or coreceptors on the host cell surface. One key feature of a virion is how many functional envelope (Env) entry spikes it has on its surface; this parameter is commonly called n_t. Likewise, T is the minimum number of spikes required for viral entry. These two terms are key to understanding the stoichiometry of neutralization because drugs or antibodies must neutralize $n_t - T + 1$ trimers in order to render a virion non-infectious. This is commonly referred to as the stoichiometry of virion neutralization [51]. The other key quantitative molecular aspect we must look at is the stoichiometry of trimer neutralization. This refers to how many gp120 subunits within a trimeric spike must be neutralized in order to impede a spike's

activity. If R5 and X4 virus differ in any of these parameters it may influence their relative entry efficiency.

There are factors, beyond the molecules used in the entry process, which are also relevant to the differences between tropism phenotypes. In addition to entry efficiency, target cell availability, target cell activation state, and negative external pressures can affect viral reproductive rates.

A wider range of cell expresses CXCR4 than CCR5. Both naive and memory cells express the X4 virus coreceptor while only memory cells express CCR5. While R5 virus dominates in early infection despite this fact, the expanded target cell population of X4 virus may account for the increased morbidity seen after tropism switching. The phenotypes could also be related to the type of cells the viruses infect; or the use of a specific chemokine coreceptor could cause a change in host cell signaling or activity. Targeting activated cells, or activating target cells, could increase the relative probability that an entry event yields a productive infection. Or, an activated cell may more efficiently produce the viral proteins and thus yield a larger viral burst size per infected cell.

Negative pressures may also play a role in R5's initial dominance. A selective pressure could disfavor X4 viral replication in early infection. It is well known that the cytotoxic lymphocyte response partially limits viral replication [52-57] and it is possible that cells expressing CXCR4 could present antigen earlier or more efficiently [58]. If the immune system exerts more control over X4 virus than R5 virus, R5 virus would have a

replication advantage in early infection [58,59]. Then, in later stages of the disease, severe immune impairment could allow for the tropism switch [60].

In summary, HIV-1 infection is still a relevant world health issue and tropism switching leads to significant increases in morbidity and mortality. Yet, while much is known about the role that coreceptors play in the viral entry mechanism, the link between the molecules used for cell entry and the pattern of R5 dominance followed by X4 takeover is unclear. This thesis will investigate several factors that have the potential to influence the phenotypic differences of R5 and X4 tropic HIV-1.

Chapter One:

Stoichiometric Parameters of HIV-1 Entry

Introduction

To infect a target cell, HIV-1 must first attach to the cell and then initiate the fusion of the viral and cellular membranes [61]. For this purpose, HIV-1 utilizes envelope (Env) glycoproteins which protrude from the surface of the virus. These glycoproteins are assembled as trimers which are visible in electron micrographs and appear as spikes on the surface of the virion. Each spike is composed of three sets of the non-covalently associated Env subunits, gp120 and gp41 [62]. In the entry process, gp120 subunits first attach to the host cell CD4, and then these CD4-activated gp120 subunits bind to chemokine receptors, either CXCR4 or CCR5, which function as co-receptors for HIV-1 [26, 27, 63, 64]. However, the stoichiometry of this process is incompletely understood. Important unanswered questions include: how many spikes must attach to CD4 molecules, how many must bind to coreceptors, and how many subunits per spike must participate in the entry process? These quantitative aspects of viral entry are relevant to the development and dosing of entry inhibitors as well as to vaccine design.

Current nomenclature classifies an HIV-1 isolate as R5 tropic if it uses the CCR5 co-receptor to enter a host cell, X4 tropic if it uses the CXCR4 coreceptor, and dual tropic (X4R5) if it can utilize either coreceptor for entry [28]. Both X4 and R5 tropic gp120 subunits bind CD4 with a K_d of 4 nM but they bind their respective coreceptors with different strengths. R5 gp120 binds CCR5 with a K_d of 4-15 nM while X4 gp120 binds CXCR4 with a K_d of 200-500 nM. X4R5 gp120 has a reduced ability to bind both coreceptors [65-69]. Target cell prevalence also differs for X4 and R5 tropic forms of HIV-1 [70]. It is possible that viruses with different tropisms require different numbers of

Env spikes to mediate entry or that disabling subunits within a trimer has different effects on X4 vs. R5 tropic viruses.

Electron microscopic studies show multiple entry spikes contacting the target cell at the same time, but these studies cannot reveal how many of the spikes are functional nor how many are actively involved in the fusion process [71]. Molecular experiments, which commonly involve measuring the relative infectivity of virions carrying a mixture of wild type and mutant gp120 subunits, provide a way to analyze the role that individual Env spikes and their subunits play in the HIV-1 entry process. However, as table 1-1 illustrates, these experiments have yielded conflicting results [51, 72-77]. This is mostly due to the different assumption each investigator makes while modeling and to sparse data for infectivity curves. Despite the efforts of several investigators, there is still no consensus regarding the quantitative aspects of CD4 or coreceptor binding. Multiple mathematical models have been used to describe the biophysical aspects of the entry process, but few of these models have been directly compared. In this study, we present two models that each use only three variables and make no assumptions about the number of functional Env spikes a virion presents. Using these models and new experimental relative infectivity curves, we have reexamined the stoichiometry of HIV-1 entry.

Results

Model selection

Mathematical models have frequently been used to estimate the stoichiometric parameters of HIV-1 entry [51, 72-79]. The basic equation that describes the relationship between relative infectivity (

a=0 then the subunits function independently and a spike loses one third of its functional activity per mutant gp120 (

(

infectivity curves, we compared the virus preparations made with and without mutant DNA. Figure 2C shows that for both Yu2 and HXB2 Envs, virus preparations generated with equal amounts of wild type vector show reduced infectivity if mutant vector is also present. This inhibitory effect is consistent with reduced functional activity of mixed trimers containing both wild type and mutant Env subunits.

Mutations affecting coreceptor binding

We first explored the effects of including gp120 subunits that were defective in binding to the CXCR4 (X4) or CCR5 (R5) coreceptors. The mutant X4 tropic virus used was incapable of supporting virus entry due to a single amino acid substitution (R308L) in the V3 region, and the equally deficient R5 tropic mutant virus had two mutations (R315G/L317S) in the V3 loop [75]. Figure 3A shows the relative infectivity curves of chimeric virus preparations including these mutant gp120 subunits [81]. Infections were carried out in primary $CD4^+$ T lymphoblasts. As illustrated in Figure 3A, chimeric viruses with a fraction of coreceptor binding-deficient gp120 subunits showed reduced infectivity. The degree of reduction was similar for representative R5 and X4 tropic viruses.

Mutations affecting CD4 binding

Similar experiments were performed with pseudoviruses carrying mixtures of wild type gp120 and gp120 with mutations affecting CD4 binding. The previously described gp120 mutation D368R was introduced into X4 tropic (HXB2) and R5 tropic (Yu2) *env* vectors. This mutation disrupts a key salt bridge involved in CD4 binding [75]. As expected, infectivity decreased as the proportion of mutant subunits increased for both

HXB2 and Yu2 viruses (Figure 3B) [81]. Interestingly, for any given ratio of wild type and mutant plasmids, relative infectivity was marginally lower for viruses with HXB2 Env than for viruses with Yu2 Env (Figure 3B), meaning that viruses with the R5 Env Yu2 may be slightly less affected by the incorporation of CD4-binding deficient gp120 subunits.

Fitting relative infectivity curves to mathematical models of the HIV-1 entry process and determining best fit

As discussed above, the shape of the relative infectivity curves reflects the stoichiometry of molecular interactions necessary for HIV-1 entry (Figure 1). Using the equations described above, we generated theoretical relative infectivity curves for all combinations of the variables:

We determined the theoretical curves' goodness of fit by calculating the residual sum of squares. To generate confidence intervals we used 10,000 bootstrap samples per experimental data set. Each of the nine points on each new curve was individually generated by randomly sampling a population of relative infectivity (RI) values that had the same mean and standard deviation as the corresponding experimental data point. Then, we determined which theoretical curve best fit each bootstrap sample. To generate a 95% confidence interval we included sets of best-fit parameters in descending order of frequency until at least 95% of bootstrap samples were accounted for. Supplemental Table 1-1 lists all of the theoretical curve parameters in the 95% confidence interval.

Because there is experimental variation, and because the number of spikes per virus (n_t) may also very, our 95% confidence interval includes many theoretical set of parameters. Thus, for ease of comparison, table 1-2 lists the stoichiometric parameters for the eight theoretical curves that best matched the experimental curves in Figure 3. The table also shows the fraction of bootstrap cases that fit to each of those top eight parameters sets and how much of the total bootstrap parameter distribution the top eight best fits account for. In the CD4 R5 data set, all parameter sets that fall in the 95% confidence interval are listed in table 1-2. In fact, 9,044 out of 10,000 of the best fit curves (for CD4 R5) had n_t=2 and T=1 values. The other data sets had more variation and thus the top eight most common results represent smaller percentages of the 10,000 bootstrap curves.

Model comparison

Figure 4 illustrates the curves from each model, incremental (*a*) and discrete (*S*), which best matched each of the four experimental data sets. In all of the data sets analyzed, the incremental (*a*) model gave better fits than the discrete (S) model. This may indicate that entry spike function is not an all or none process and that an incremental model is more accurate.

Best fitting stoichiometric parameters

The most striking result is that entry appears to only require one or two functional spikes. As seen in Figure 1, the number of spikes required for entry (*T*) has a large impact on the shape of a theoretical relative infectivity curve. Figure 1-5 is a graphical representation of the data in supplemental table 1-1. Each bubble on the plots represents a parameter pair (n_t, *T*) and the size of the bubble is proportional to the fraction of bootstrap samples that parameter pair fits. This analysis shows that very low values of *T* most frequently generated theoretical curves that matched the experimental data. Similarly, our better fitting model, the incremental (*a*) model, suggests that the number of functional spikes/virion (n_t) is also low (2-4) (Figure 1-5 A-D).

For coreceptor binding, both HXB2 (X4) and Yu2 (R5) viruses consistently utilize only one or two entry spikes. For YU2 entry into primary $CD4^+$ T cells, our experimental results are consistent with a model in which a single functional spike is sufficient for entry and within that spike there is a moderate level of subunit interdependence. The HXB2 coreceptor binding data matches a model in which either one or two spikes are necessary.

During the CD4 binding stage of the entry process, HXB2 viruses again appear to require only one or two spikes to attach to the target cell while YU2 more clearly requires only one. It is interesting to note that if two spikes are engaged, then fewer active subunits per spike are required.

According to the discrete (*S*) model, there is no difference between HXB2 (X4) and YU2 (R5) virus entry stoichiometry. While the HXB2 and YU2 parameter values in the confidence intervals of the incremental (*a*) model do overlap, HXB2 (X4) virus seems more likely to require two spikes than YU2 (R5).

Discussion

In this paper, we present experimental relative infectivity curves which elucidate the stoichiometry of CD4 and coreceptor binding during HIV-1 entry. Several previous reports have also investigated the entry stoichiometry HIV-1 [51, 72-78]. However, it is difficult to directly compare the results of our study with those of other studies due to differences in experimental design and modeling assumptions. Our study, however, has several strengths; each relative infectivity curve was generated with nine different pseudovirus preparations carrying different ratios of wild type to mutant gp120 subunits. Because of the number of points per curve, our analysis has substantial predictive power that enables us to use equations with three variables. In addition, we used two different types of mutants (specific to either CD4 or coreceptor binding). Table 1-1 compares nine stoichiometry studies, their assumptions, methods, and experimental findings. Figure 1-6 compares our experimental data with the theoretical curves that correspond to some of the parameters suggested by other groups in table 1-1.

A striking finding in the present study is the low number of functional spikes per virion (n_t). Other authors have reported similar observations but the results have been controversial [74-77]. One reason for the controversy is that electron tomography studies appear to present a different picture. They show more than 1-3 spikes on the surface of a virion, and they show HIV-1 Env trimers clustering together on the virion surface to form "entry claws" [71]. An alternate interpretation of n_t is that each "entry claw" has only two or three functional spikes and the clustering of spikes serves to increase the probability that the minimum number of functional Env trimers will contact a cell. Additionally, a virus is roughly spherical, and spikes that are not positioned or grouped close enough to

the site of cell contact may not be relevant to the entry process. Thus our finding that n_t is low may not mean that there are only 2-3 entry spikes on a virion, but rather that there are between 2 and 3 entry spikes that can, on average, simultaneously contact a target cell's receptors.

Conclusion

Our study confirms that HIV-1 entry requires only one or two functional Env entry spikes. It also concludes that an individual virion, on average, has either two or three spikes on its surface that are both functional and able to simultaneously contact a target cell. In addition, our analysis shows that Env trimers may function with fewer than three active subunits. Subunit interaction is best modeled using an incremental variable, and this indicates that subunit and entry spike function is not an all or none process. These observations together do not paint an optimistic picture for vaccine development; in order to disable a virion, a drug or antibody needs to bind nearly all of the subunits on all of the Env spikes. Finally, our analysis indicates that, at least in reference to entry stoichiometry, there is at most a minimal biophysical difference between HXB2 (X4 tropic) and Yu2 (R5 tropic) viruses. The collections of best fit parameters for each virus overlap each other.

Methods

Mutants

We used a total of four different *env* mutants to make chimeric viruses that express both wild type and mutant gp120. Previously characterized mutations that prevent binding to CD4 (D368R) or to coreceptors (R308L or R315G/L317S) [19] were introduced into the reference isolates HIV-1HXB2 (X4 tropic) and HIV-1Yu2 (R5 tropic) using the Quick Change Sight–Directed Mutagenesis Kit (Invitrogen, Grand Island, NY). While the reference isolates express the entire gp160 protein, in this paper we discuss the results in terms of gp120 because only the gp120 portion is affected by the mutations and is involved in the binding events of interest.

Generating Chimeric Virus

Relative infectivity assays were performed with pseudotyped virions that carry heterotrimers of HIV-1 Env proteins composed of wild-type gp120 subunits and gp120 subunits that are defective in either CD4 or coreceptor binding. The assembly and virion incorporation of such heterotrimers has been confirmed previously [74, 79, 80]. We produced these chimeric pseudotyped viruses, which are capable of only single-round infection, as previously described [56]. Briefly, we transfected HEK293T cells with a GFP-tagged, Env-defective HIV-1 proviral vector (pNL43-ΔE-EGFP) and either with a wild type HIV-1 Env expression vector (HIV-1HXB2 or HIV-1Yu2) or with a mixture of wild type and mutant Env expression vectors. By varying the ratio of wild type and mutant DNA in the transfection mixture, we controlled the relative abundance of wild

type and mutant gp120 subunits in the viral entry spikes. Nine ratios of wild type env DNA: mutant env DNA were used, ranging from 9:1 to 1:9. Transfections were carried out using Lipofectamine 2000 (Invitrogen, Grand Island, NY) according to the manufacture's protocol. The media was replaced six hours after transfection, and cells were incubated at 37ºC for an additional 48 hours before the virus containing supernatant was added to target cells.

Single-round relative infectivity assay

We used a modified single-round infectivity assay to assess the effect of mutant Env subunits on infectivity as previously described [65]. Briefly, peripheral blood mononuclear cells were obtained from healthy blood donors by Hypaque-Ficoll gradient centrifugation and then activated with phytohemagglutinin (0.5 µg/ml) and interleukin-2 (100 U/ml) for 3 days. $CD4^+$ T cells were isolated by negative selection using antibody coated magnetic beads (Miltenyi, Bergisch Gladbach, Germany) and seeded into a 96-well plate at 1×10^5 cells per well in RPMI1640 supplemented with 10% fetal bovine serum, interleukin-2 (100 U/ml) and cytokine-rich supernatant. Cells were infected using fresh pseudovirion preparations. To each well, 5-20 µl of virus containing supernatant was added (sufficient to produce 1-20% infection) and cells were infected by spinoculation at 1,200*g*, 30°C for 2 hours and further incubated at 37°C for 3 days. All experiments were done in triplicate with cells from at least three different donors, and virus from at least three different preparations.

After the 3 day incubation, cells were washed, resuspended, and fixed with 3% formaldehyde. We quantified infectivity as the percentage of GFP^+ cells by FACS

analysis (FACS Calibur, BD Bioscience) [82]. All replicates, not means or medians, were used in the curve matching and statistical analysis. All healthy blood donors gave their written informed consent, and the study was approved by the Institutional Review Board of Johns Hopkins University.

Western blots

For the analysis of HIV-1 gp120 expression, 293T cells were transfected as described above with constant amounts of NL43 DNA and varying amounts of vectors containing either wild type or mutant *env*. After 48 hours of virus production time, the HIV-1 rich supernatants were collected without disturbing the 293T cells. Samples were prepared with NuPAGE LDS sample buffer according to manufactures instructions (Invitrogen, Grand Island, NY) and 40ul of each was loaded and electrophoresed on a NuPAGE 4-12% Bis-tris gell (NOVEX, Grand Island, NY) and then transferred to an Immun-Blot PVDF membrane (Bio Rad, Hercules, CA). The blots were first probed with a primary antibody to HIV-1 gp120 (abcam, Cambridge, UK) and then a horseradish peroxidase-conjugated rabbit anti- goat antibody was added. The secondary antibody was detected through autoradiography using enhanced chemiluminescence.

Curve matching

After FACS analysis, the percent relative infection (

30); *T,* the number of spikes required for entry (range T = 1-30), and either *a,* a measure of subunit interdependence (a continuous variable, range a = -0.5-1, calculated at 0.1 intervals); or *S,* a measure of the ability of individual subunits to compensate for each other (a discreet variable with possible values 1, 2, 3). The shape of a relative infectivity curve reflects the stoichiometry of the biological process, and altering any of these parameters changes the shape of the predicted curve (Figure 1). The program compared each theoretical curve to each experimental

Table 1-1: A simplified summary of HIV-1 stoichiometry studies.

	Assumption	Points per infectivity curve	Experimental findings	Target cell studied	Method used
Kuhman 2000	n_t *and S not accounted for*	*NA*	*T=2-6*	HeLa CD4 cells	Used mutations that reduced viral CCR5 binding ability and monitored infectivity relative to coreceptor expression levels
Yang 2005a	n_t *not accounted for* S=1	6	*T*=1	Cf2Th-CD4/CCR5 cells	Mixing gp160 cleavage mutant or fusion peptide mutant and wild type *env*, luciferase reporter
Yang 2005b	n_t *not accounted for*	3	*T*=1 *S*=1	Cf2Th-CD4/CCR5 cells	Mixing antibody sensitive and resistant *env*, luciferase reporter
Yang 2006	n_t *not accounted for T=1*	4	*S*=2	Cf2Th-CD4/CCR5 cells	Mixing coreceptor/CD4 binding mutant and wild type *env*, luciferase reporter
Herrera 2006 -2nd model	n_t = 9 S=1 n_t *and T not accounted for*	5	R5: *T*=4 X4:*T*=5 R5: *a*=1 X4: *a*=.365	U87. CD4.CCR5 and U87.CD4.CX CR4 cells	Mixing gp160 cleavage mutant with wild type *env*,
Klasse 2007	n_t = 9	*No new data*	*S*=1 *T*= 4-5	NA	Uses Yang 2005a, 2005b, 2006 and Herrera 2006 data
Mangus 2009	n_t = 14±7 *S=1*	*No new data*	*S*=1 *T*=2-9	NA	Uses Yang 2005b data
Mangus 2010	n_t = 14±7 *T=8*	*No new data*	*S*=1 *T*=8	NA	Uses Yang 2005a data
This study 2013	None	9	n_t =1-3 *T*=1-2 *S*=1-2 *a*=varied	Primary $CD4^+$T cells	Mixing coreceptor/CD4 binding mutant and wild type *env*, GFP reporter

Table 1-2: The stoichiometric parameters yielding the best fitting theoretical relative infectivity curves. The % column shows the fraction of the bootstrap parameter distribution that each individual set of parameters represents. The Total % column shows how much of the total bootstrap parameter distribution the top eight best fits account for.

		Incremental *"a" model*					**Discrete *"S" model***				
Mutation	**Viral Tropism**	n_t	***T***	***a***	**%**	**Total %**	n_t	***T***	***S***	**%**	**Total %**
Coreceptor	X4	2	1	0.8	29%	87%	3	1	1	26%	76%
		2	1	0.7	22%		5	3	2	13%	
		3	2	0.4	14%		3	2	2	10%	
		3	2	0.5	12%		2	1	1	9%	
		2	1	0.6	5%		4	1	1	9%	
		3	2	0.6	5%		6	4	2	5%	
		4	3	0.5	1%		4	2	2	4%	
Coreceptor	R5	2	1	0.6	20%	76%	4	2	2	15%	57%
		2	1	0.5	17%		5	2	2	8%	
		2	1	0.7	16%		3	1	1	8%	
		2	1	0.4	10%		2	1	2	7%	
		2	1	0.8	5%		4	1	1	7%	
		2	1	0.3	5%		3	1	2	6%	
		3	2	0.4	2%		6	3	2	6%	
CD4	X4	3	2	0.4	19%	70%	3	1	1	24%	70%
		3	2	0.5	15%		3	2	2	11%	
		3	2	0.3	13%		2	1	1	11%	
		3	2	0.6	8%		4	1	1	8%	
		2	1	0.8	6%		5	3	2	6%	
		3	2	0.2	5%		6	4	2	5%	
		2	1	0.7	3%		7	2	1	4%	
CD4	R5	2	1	0.5	31%	96%	4	2	2	25%	70%
		2	1	0.6	29%		5	2	2	12%	
		2	1	0.4	16%		3	1	2	8%	
		2	1	0.7	10%		5	1	1	7%	
		2	1	0.3	4%		4	1	1	7%	
		3	2	-0.1	3%		6	1	1	6%	
		3	2	-0.2	2%		7	3	2	5%	

Figure 1-1

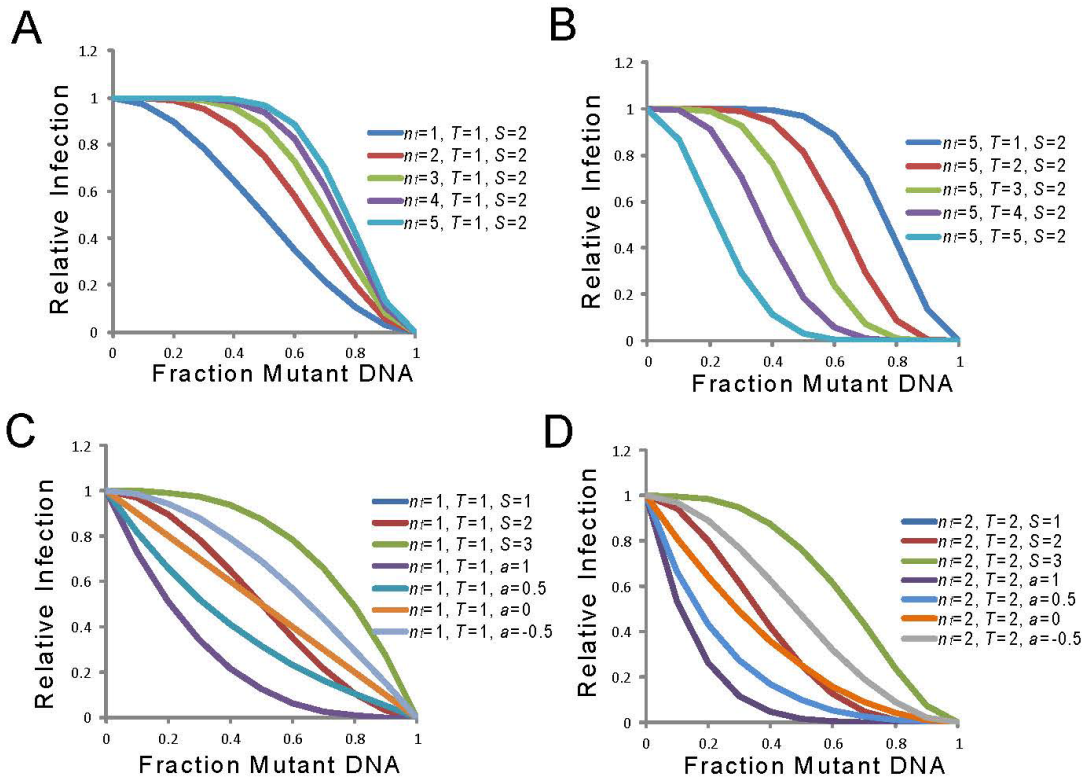

Figure 1-1. Theoretical relative infectivity curves generated using various combinations of HIV-1 entry stoichiometric parameters. The relative infectivity curves representing the results from theoretical systems with various stoichiometric parameters. The y-axis is the relative infectivity or the virus and the x-axis is the fraction of mutant DNA used is virus generation (P_f). The equations were solved for fractions of mutant DNA from 0 to 1 at 0.1 intervals and graphed as solid lines. **A**: The effect of varying n_t. In this example, n_t =1-5, T=1 and S=2. **B**: The effect of varying T. The n_t values are held constant at 5 and T ranges 1-5. **C and D**: The effect of altering S and a. Note that S=1 lines are not visible because they are identical to a=1.

Figure 1-2

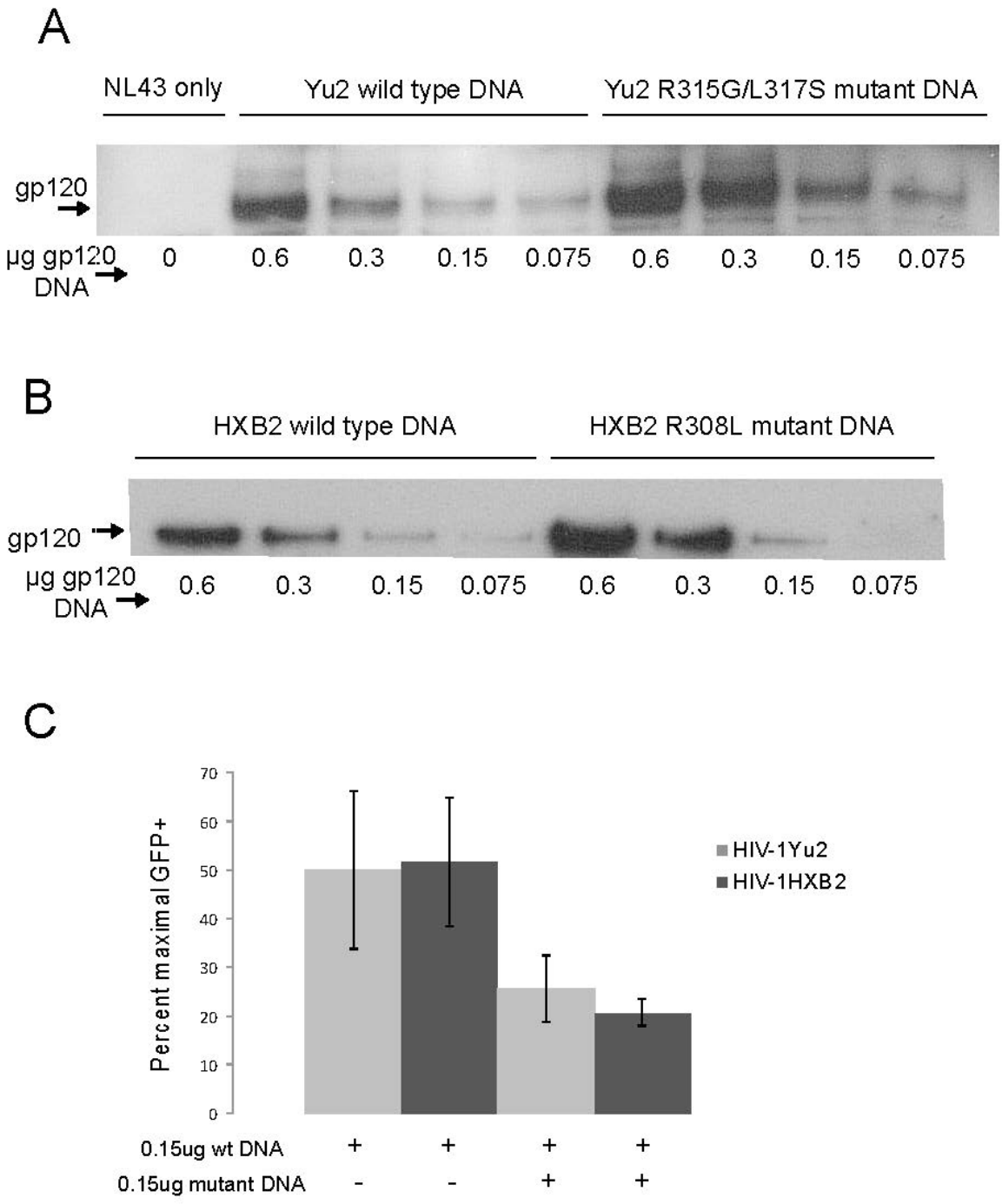
A
NL43 only
Yu2 wild type DNA
Yu2 R315G/L317S mutant DNA
gp120
µg gp120 DNA
0
0.6
0.3
0.15
0.075
0.6
0.3
0.15
0.075
B
HXB2 wild type DNA
HXB2 R308L mutant DNA
gp120
µg gp120 DNA
0.6
0.3
0.15
0.075
0.6
0.3
0.15
0.075
C
Percent maximal GFP+
70
60
50
40
30
20
10
0
HIV-1Yu2
HIV-1HXB2
0.15ug wt DNA
0.15ug mutant DNA
+
+
+
+
-
-
+
+

Figure 1-2. Immunoblots and relative infectivity curve illustration gp120 production and incorporation. A and B: Western blots showing the gp120 band. Equal amounts of virus containing supernatants were loaded. Viruses were generated using 0.6 μg of pNL4-3Δ*env* DNA and the indicated amounts of expression vectors for the Env proteins from HIV-1Yu2 (A) or HIV-1 HXB2 (B). **C:** Relative infectivity of virus preparations made with equal amounts of wild type Env expression vectors, with or without mutant Env expression vectors. Results are expressed as percent of maximal infection achieved with 0.3 μg wild type vector.

Figure 1-3

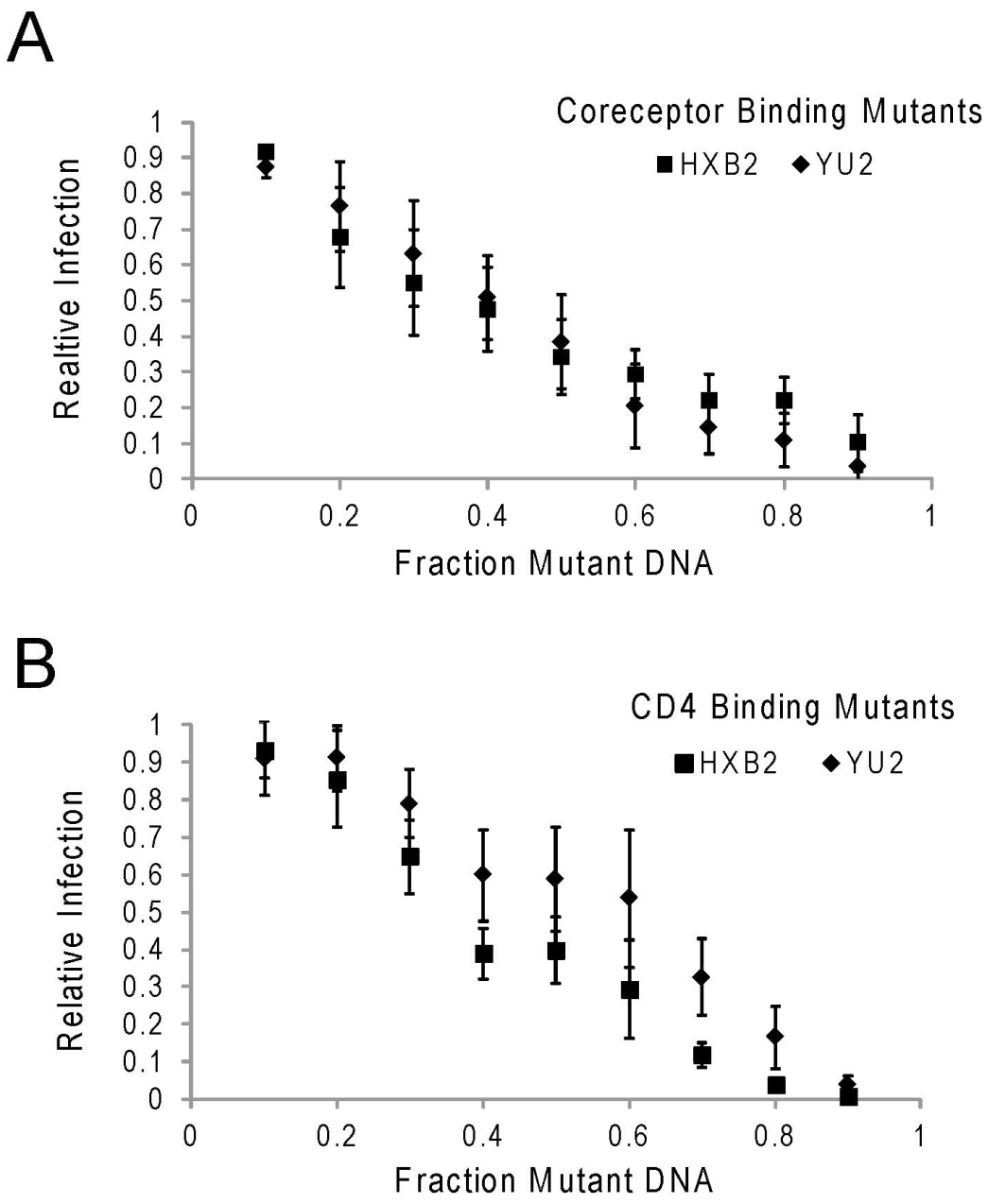

Figure 1-3. Relative infectivity curves comparing HIV-1HXB2 (X4) and HIV-1Yu2 (R5) viruses. A and B: Relative infectivity curves, the fraction of mutant DNA indicated was used in virus production. **A**: HIV-1Yu2 R315G/L317S mutant or HIV-1HXB2 R308L mutant DNA. **B**: D368R mutant DNA, HIV-1HXB2 or HIV-1 Yu2.

Figure 1-4

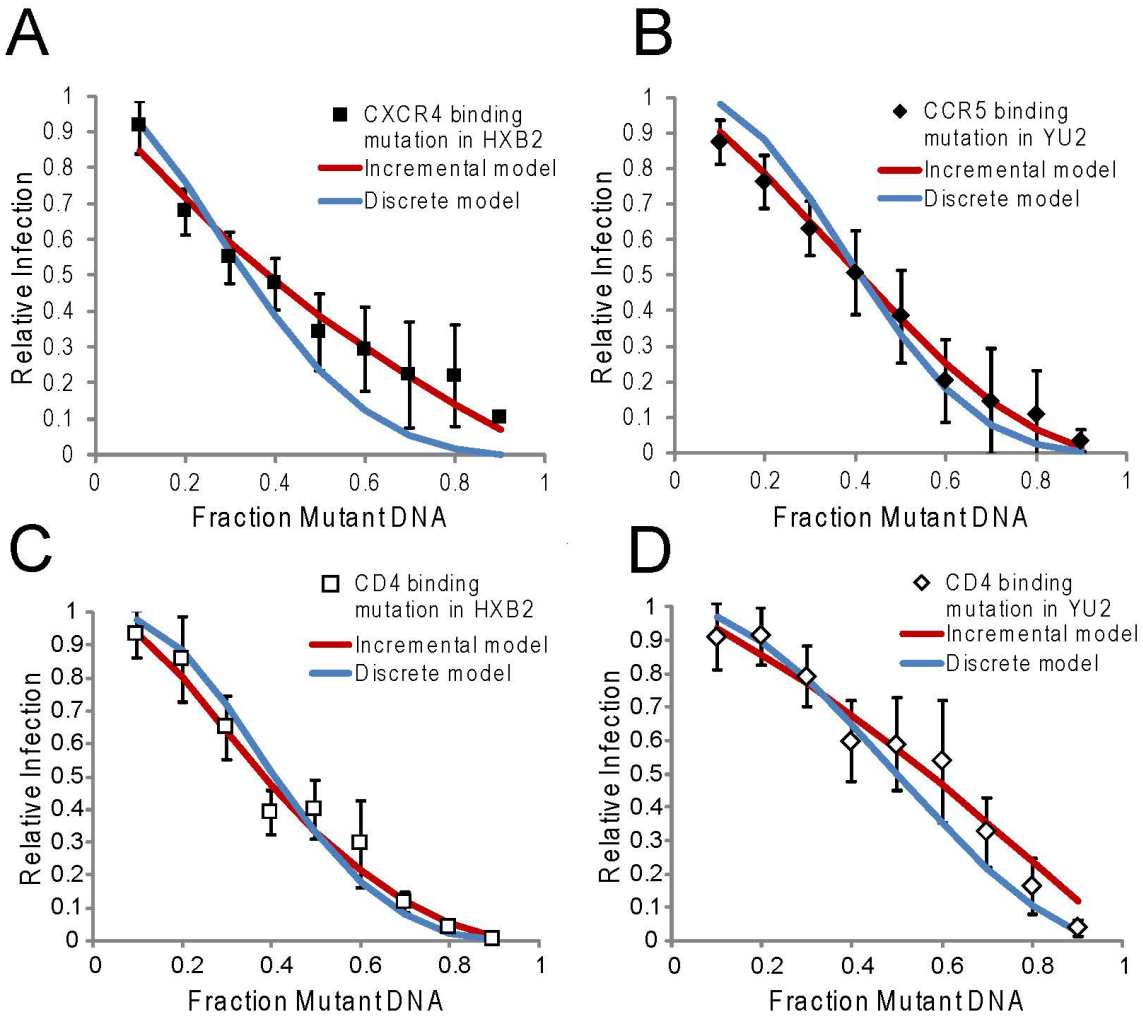

Figure 1-4. Relative infectivity curves demonstrating the fitting of the theoretical models. Experimental relative infectivity data for HXB2 (A, C, squares) and Yu2 (B, D ,diamonds).Virus preparations made with increasing fractions of mutant vectors encoding Env protein defective in coreceptor binding (A, B, solid symbols) or CD4 binding mutant (C, D, open symbols). Experimental data are compared to the theoretical relative

infectivity curves (colored lines) from the incremental (red) or discrete (blue) models that best fit the experimental data. (A) HIV-1HXB2 R308L mutant, incremental model: n_t=1 T=1 a=0.3; discrete model: n_t=2 T=1 S=1. (B) HIV-1Yu2 R315G/L317S mutant, incremental model: nt = 2, T = 2, a = -0.3; discrete model: nt = 3, T = 1, S = 1. (C) HIV-1HXB2 D368R mutant, incremental model: nt= 0.3; discrete model: nt = 3, T = 1, S = 1. (D) HIV-1Yu2 D368R mutant, incremental model: nt= 1, T = 1, a = -0.2; discrete model: nt = 1, T = 1 S = 2.

Figure 1-5

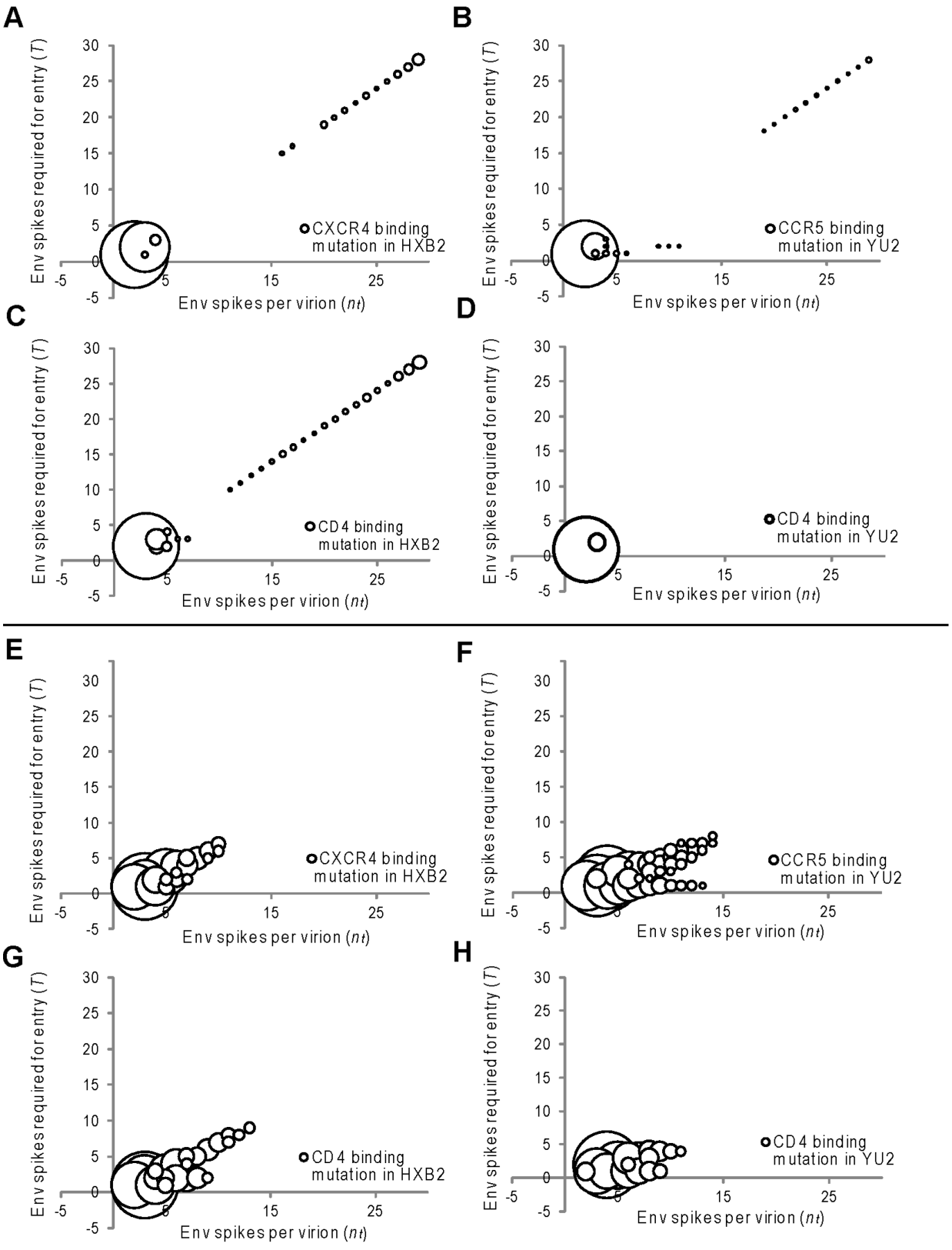
A
B
C
D
E
F
G
H
Env spikes required for entry (T)
Env spikes per virion (nt)
CXCR4 binding mutation in HXB2
CCR5 binding mutation in YU2
CD4 binding mutation in HXB2
CD4 binding mutation in YU2

Figure 1-5 Bubble graphs illustrating the best fitting n_t and T values. Each point on a graph represents a parameter pair with n_t on the x-axis and T on the y-axis. The size of the point is proportional to the fraction of bootstrap samples that parameter pair fit best. Graphs A-D show the fitting results from the incremental (*a*) model and graphs E-H show the discrete (*S*) model. Supplemental table 1-1 lists the values presented on these graphs and also the corresponding *a* and *S* values.

Figure 1-6

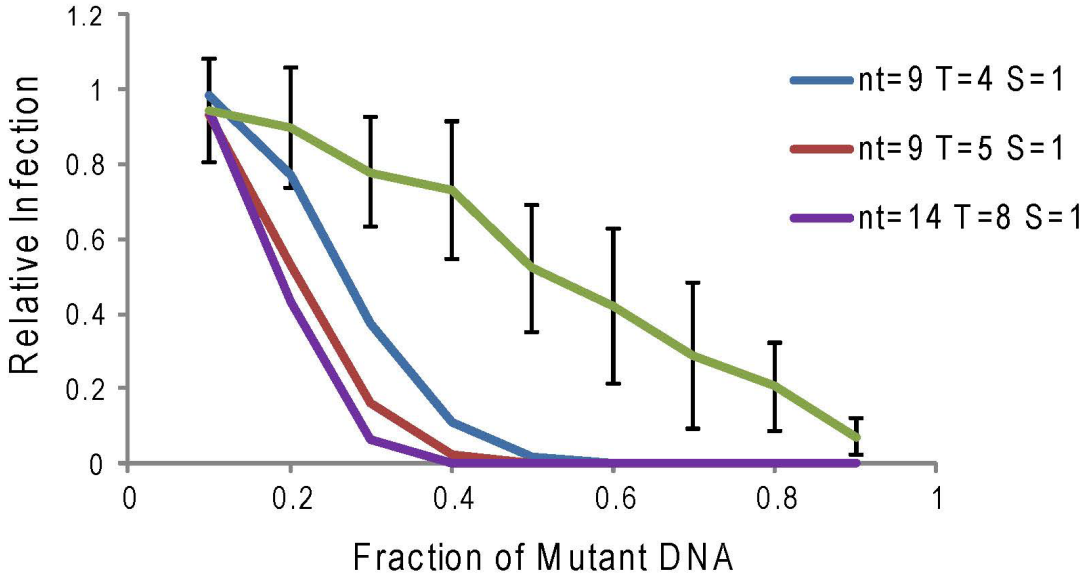

Figure 1-6. Theoretical curves matching parameters listed in Table 1-1. The green line with error bars is the CCR5 binding mutation in Yu2 line from Figure 1-3 A. The blue red and purple lines are the theoretical curves that our model generates using a few of the parameters predicted by other groups who began their calculation with an assumption that there are 9 (blue and red lines) or 14 (purple line) spikes on a virion.

Supplemental Table 1-1 A list of all the bootstrap parameter sets that fall within a 95% confidence interval. The column "# best fits" is the number of times, out of 10,000 trials, that a set of parameters best fit a bootstrap generated experimental data set.

CXCR4 binding mutation in HXB2

n_t	T	a	#best fits
2	1	0.8	2872
2	1	0.7	2225
3	2	0.4	1383
3	2	0.5	1211
2	1	0.6	468
3	2	0.6	458
4	3	0.5	98
2	1	0.9	62
3	2	0.7	52
29	28	0.9	52
2	1	0.5	40
29	28	0.5	36
28	27	0.5	31
22	21	0.4	31
20	19	0.4	29
27	26	0.5	28
29	28	0.6	26
24	23	0.4	25
3	1	0.9	24
28	27	0.7	23
26	25	0.4	23
28	27	0.6	22
27	26	0.4	22
29	28	0.4	22
21	20	0.4	21
20	19	0.5	21
4	3	0.6	21
28	27	0.4	20
29	28	0.8	20
3	2	0.1	20
23	22	0.5	19
24	23	0.5	19
16	15	0.4	18
3	1	0.8	18
17	16	0.4	17
27	26	0.6	17

CCR5 binding mutation in YU2

n_t	T	a	#best fits
2	1	0.6	2011
2	1	0.5	1696
2	1	0.7	1642
2	1	0.4	1033
2	1	0.8	509
2	1	0.3	470
3	2	0.4	214
2	1	0.2	184
3	2	-0.1	175
3	2	0.5	174
3	2	0	136
3	2	-0.2	115
3	2	0.1	101
3	2	0.6	70
2	1	0.1	65
3	2	-0.3	63
3	2	0.3	51
3	2	0.2	40
5	1	0.9	36
4	1	0.9	27
3	1	0.7	27
4	1	0.8	26
3	1	0.8	24
6	1	0.9	21
3	1	0.6	20
3	2	-0.4	20
29	28	0.9	18
4	2	-0.1	18
4	3	-0.3	18
24	23	0.4	17
9	2	0.8	15
23	22	0.4	15
20	19	0.4	14
29	28	0.7	14
2	1	0	14
25	24	0.4	13

25	24	0.4	17
28	27	0.5	12
27	26	0.5	12
21	20	0.4	11
10	2	0.8	11
11	2	0.9	11
3	1	0.9	11
4	3	0.5	11
19	18	0.4	11
22	21	0.5	10
22	21	0.4	10
23	22	0.3	10
29	28	0.5	10
26	25	0.4	10
26	25	0.6	10

CD4 binding mutation in HXB2

n_t	T	a	#best fits
3	2	0.4	1938
3	2	0.5	1486
3	2	0.3	1317
3	2	0.6	812
2	1	0.8	594
3	2	0.2	510
2	1	0.7	303
4	3	0.5	178
4	3	0.4	144
29	28	0.9	144
3	2	0.1	136
4	2	0.6	123
4	2	0.5	121
4	3	-0.1	102
4	3	0	94
2	1	0.9	90
5	2	0.7	71
3	2	0.7	69
4	3	0.6	42
4	2	0.7	41
4	3	-0.2	40
2	1	0.6	38
20	19	0.4	35
5	2	0.8	34
24	23	0.4	31
28	27	0.7	30

CD4 binding mutation in YU2

n_t	T	a	#best fits
2	1	0.5	3138
2	1	0.6	2850
2	1	0.4	1633
2	1	0.7	980
2	1	0.3	443
3	2	-0.1	269
3	2	-0.2	183
3	2	0	110

16	15	0.5	29
4	3	0.1	29
27	26	0.4	29
3	2	0	29
17	16	0.4	28
28	27	0.6	28
5	4	0.5	26
6	3	0.5	26
27	26	0.5	26
7	3	0.6	25
29	28	0.6	25
28	27	0.5	24
27	26	0.6	24
4	2	0.4	24
23	22	0.4	23
24	23	0.5	23
29	28	0.5	23
5	4	-0.2	22
22	21	0.5	22
15	14	0.4	22
21	20	0.4	21
16	15	0.4	21
21	20	0.5	21
24	23	0.3	21
28	27	0.9	20
26	25	0.4	20
3	1	0.9	20
28	27	0.8	19
28	27	0.4	19
18	17	0.4	19
14	13	0.4	19
29	28	0.8	19
29	28	0.4	19
13	12	0.4	19
27	26	0.8	18
5	4	-0.3	18
29	28	0.7	18
22	21	0.4	16
12	11	0.4	16
25	24	0.4	16
23	22	0.5	15
27	26	0.7	15
11	10	0.4	15

19	18	0.4	15
25	24	0.6	15
17	16	0.5	14
5	2	0.6	14

CXCR4 binding mutation in HXB2

n_t	T	S	#best fits
3	1	1	2629
5	3	2	1279
3	2	2	957
2	1	1	922
4	1	1	886
6	4	2	540
4	2	2	404
2	1	2	330
8	5	2	284
7	4	2	255
9	6	2	176
7	5	2	158
5	1	1	137
6	2	1	124
10	7	2	105
5	2	1	85
10	6	2	67
7	2	1	62
6	3	2	56
9	5	2	55

CCR5 binding mutation in YU2

n_t	T	S	#best fits
4	2	2	1529
5	2	2	764
3	1	1	754
2	1	2	735
4	1	1	705
3	1	2	611
6	3	2	569
5	1	1	502
5	3	2	345
6	1	1	330
7	1	1	220
7	3	2	211
7	4	2	191
8	4	2	173
6	2	2	147
2	1	1	138
8	1	1	138
3	2	2	130
9	5	2	101
9	4	2	101
9	1	1	92
8	3	2	85
10	5	2	80
12	6	2	67
11	6	2	67
10	4	2	65
11	5	2	57
10	6	2	51
10	1	1	49
8	5	2	48
4	1	2	46
11	4	2	38
11	1	1	35
9	3	2	34
12	5	2	34
13	7	2	32

7	2	2	29
12	1	1	28
13	6	2	27
12	7	2	27
10	3	2	22
6	4	2	21
11	7	2	19
14	8	2	18
14	7	2	18
13	1	1	13
8	2	2	13

CD4 binding mutation in HXB2

n_t	T	S	#best fits
3	1	1	2442
3	2	2	1141
2	1	1	1094
4	1	1	813
5	3	2	603
6	4	2	476
7	2	1	406
6	2	1	385
9	6	2	242
8	2	1	222
4	2	2	192
10	7	2	192
8	5	2	179
5	2	1	158
7	5	2	134
5	1	1	131
4	3	2	131
11	8	2	110
4	2	1	84
11	7	2	74
2	1	2	73
12	8	2	64
7	4	2	64
13	9	2	60
9	2	1	51

CD4 binding mutation in YU2

n_t	T	S	#best fits
4	2	2	2474
5	2	2	1194
3	1	2	817
5	1	1	689
4	1	1	670
6	1	1	614
7	3	2	541
6	3	2	535
7	1	1	370
3	1	1	304
8	4	2	221
9	4	2	209
8	3	2	200
8	1	1	179
2	1	2	171
10	4	2	114
6	2	2	99
9	1	1	97
11	4	2	48

Chapter Two:

Investigating Possible Causes for R5 Tropism Dominance in Early Infection and Tropism Switching in Advanced Disease

Introduction

To attach to and enter a host cell, human immunodeficiency virus type 1 (HIV-1) must bind a CD4 receptor on the target cell surface. After the virus attaches to the CD4 molecule, it then binds a coreceptor to complete the entry process. Viruses that use the chemokine coreceptor CCR5 are commonly called R5 tropic viruses and those that use CXCR4 are named X4 tropic viruses [28]. While much of the sequence difference between the viral genomes of R5 and X4 tropic virus has been examined and described, we lack a definitive explanation for the virus's phenotypic differences.

Usually, new infections arise from only one or very few genotypic species [83-40]. Interestingly, the transmitter founder virus is almost always R5 tropic; this is true for sexual transmission, parenteral, and vertical transmissions [39]. After infection is established, the virus evolves and diversifies quickly, driven by its high rate of replication, mutation, and recombination [86-88]. In approximately 50% of HIV-1 subtype B infected patients, in late stages of disease, the virus evolves away from its initial CCR5 binding preference and switches to CXCR4 usage [28, 77, 89-93]. This switch in dominant viral tropism is associated with accelerated $CD4^+$ T cell depletion as well as increased morbidity and mortality [35, 82, 94-99].

Any hypothesis that aims to explain the phenotypic differences between R5 and X4 HIV-1 virus must account for both the initial R5 dominance and the switch to X4 (is seen in ~50% of patients). One of the most common explanations, preferential transmission, falls short here. It cites random mutation as the cause of the latter and the observed bottle neck effect that passing through a CCR5 coreceptor rich mucosal

membrane during sexual transmission has on an HIV-1 virus population as the cause of the former. But the preferential transmission explanation is undermined by the fact that R5 dominance is transmission route independent [36, 27, 100, 101]. Infections originating from intravenous drug use and blood transfusions also show R5 dominance [39], as do IV infected monkeys [102] and needle stick victims [45, 103].

Another potential explanation, the immune-control hypothesis, posits that the immune system exerts more control over X4 virus than R5 virus, and thus R5 virus has a replication advantage in early infection [58, 59]. Then, a severe immune impairment allows for the tropism switch [60]. Callaway, *et al.,* confirmed the theoretical potential of this hypothesis with a complex model of viral dynamics that predicts tropism switching in a manner that is consistent with experimental and clinical observations [104]. Their analysis shows that a strong immune system with enhanced ability to recognize X4 virus is sufficient to select for an R5 virus while a weak immune system favors X4 propagation. Additionally, Bonhoeffer, *et al*., conclude that the ratio of nucleotide substitutions per synonymous site, (d_s) to non-synonymous site (d_n) is significantly lower in X4 tropic strains [58]. Low d_s/d_n ratios indicate strong diversifying selection for amino acid change and Bonhoeffer, *et al.,* note that their results could be explained by an immune system that more strongly affects X4 virus [58]. It is well known that the cytotoxic lymphocyte response partially limits viral replication [52-57] and it is possible that cells expressing CXCR4 could present antigen earlier or more efficiently [58]. Supporting experimental evidence for this hypothesis comes from two animal studies which implicate the cytotoxic lymphocyte (CTL) as the component of the immune system specifically controlling X4 tropic virus [102, 105].

A third theory explains R5 dominance and tropism switching with a combination of differing replication rates and target cell availability. This hypothesis posits that R5 virus has some replication advantage in early infection that either disappears or is outweighed by target cell availability in later infection. Changes in the target cell population over time will affect the relative fitness of the viral tropisms. R5 and X4 have overlapping but different target cell populations. Because X4 virus has a wider target cell range, the relative fitness of X4 virus will as a dominant R5 virus depletes its target cell population, [106- 108]. Several mechanisms for R5 virus's replication advantage are possible: (1) R5 virus may have a larger burst size; producing more virus particles per infected cell could mean a higher R_0. (2) R5 virus may have the ability to enter cells more efficiently than X4. This would give R5 a replication advantage until its target cells are depleted. (3) R5's early competitive advantage could be target cell related and come from a compartment where cells express CCR5 but not CXCR4. The gut associated lymphoid tissue (GALT) could be such a location as it is CCR5 rich and its cells are often the first to be depleted regardless of the infection rout [109]. (4) The activation state of the cells each virus infects could affect the percentage of entry events that lead to productive infection. Naïve CD4+ T cells express CXCR4 while memory CD4+ T cells express both CXCR4 and CCR5 [106]. In early infection, memory cells proliferate up to ten times as frequently as naive cells and it is only in late infection that the proliferation rates even out [110]. Thus, in early infection, X4 entry is less likely to produce a productive infection [101, 111]. In fact, Weinberger, *et al*., present a mathematical model that concludes that an increase in the ratio of the fractions of activated memory and naive CD4+ T cells, as

occurs when the CD4+ T cell concentration drops below a threshold, is sufficient to produce a tropism switch [112].

To further investigate the immune-control hypothesis and the replication rate/target cell availability hypothesis we conducted a range of experiments with a panel of viruses of varied tropisms. We explore CTL suppression of infection as well as burst size, infection kinetics, and target cell populations.

Results

Tropism characterization: Traditionally, when studying viral tropism, standard reference strains like YU2 (R5) and HXB2 (X4) are used. But because the sequences of these strains also differ in areas not associated with coreceptor specificity, the comparison is not perfectly controlled. In order to focus on tropism specific differences we used a series of viral Env clones, ranging from R5 to X4 tropic, that all came from the same patient [113]. The clones were longitudinally collected by Shankarappa, *et al*., from their study patient number five whose virus was originally R5 tropic and then switched to X4 tropic at 5.67 years post infection [77, 114]. These Env expressing plasmids were kindly donated to us by Coetzer, *et al*.

The tropisms of the six clones used in this study are listed in Figure 2-1A, along with their numerical designation from Shankarappa, *et al*., and the year post infection that they were isolated. Figure 1B shows the relative inhibition of each clone by the coreceptor binding drugs AMD3100 (CXCR4) and Maraviroc (MVC, CCR5). The results presented here are similar to the characterizations made by Coetzer, *et al*. Extensive sequence analysis of these clones has been conducted previously [113]. For visual comparison purposes, Figure 2 shows the variable loop regions, which contribute most to the increased diversity at 5.67 years post infection.

Infectivity: Figure 3 shows infectivity graphs for the six viruses in $CD4^{+}$T cells from two different representative healthy donors. For the same amount of concentrated virus, the X4 tropic clones infect more cells than the R5 viruses do. The p24 concentrations of the virus preparations were also tested and were all within experimental error of one another

(data not shown). Thus, while the X axis is labeled as "Concentrated virus (ul)," the volume corresponds to the p24 added.

The tropism specific differences in infectivity shown here may be attributable to coreceptor availability. Figure 4 shows the specific antibody binding capacity of a $CD4^+$T cell for CD4, CXCR4, and CCR5 antibodies. This FACS based assay uses a standard curve, made from beads with known numbers of antibody binding sights (figure 4B), to convert a sample's mean florescence intensity into antibody binding units. While all of the cells express CD4 and CXCR4, only 8.7% of cells express measurable numbers of CCR5 coreceptors (figure 4A).

Burst Size: The burst size of a cell infected by one of the six viral clones was calculated by first assessing the total p24 output of a well of cells via p24 ELISA and then dividing that by the percent of cells with productive infections. Because the difference between the individual donors was often larger than the difference between viral clones the data was further normalized with the largest burst size of each donor set to one. Figure 5 shows the average relative burst sizes of five donors. While there are differences between the viral clones, no tropism related pattern appears.

Suppression: In the suppression assays, the variation in infectivity between donors persisted and thus we chose to show three individual representative donors instead of an average. The left three graphs in figure six show the dose response relationship between the percentage of $CD4^+$ T cells infected and the ratio of $CD8^+$ effector cells. $CD8^+$ T cells clearly cause suppression of infection, as seen by %GFP. However, this format does not

allow for an easy comparison among the six virus types. The calculated levels of suppression, shown in the right hand column, are the result of subtracting the percent GFP of the CD4's that were in contact with CD8's from the CD4 only percent infection, and then dividing by the former. There was no correlation between tropism and suppression from CD8's.

Modeling growth kinetics: Equation 1 describes the rate of change of viral load where

the single round, *in vitro* assay viral clearance is not relevant. Equation 2 does not include the term for infected cell death (

Discussion

Tropism characterization: Each isolate in this study was affected by only one of the two entry inhibitors, AMD3100 or Maraviroc. While including perfectly dual tropic virus in the study would have been ideal, it is not surprising that this was not possible. Dual tropic virus has a decreased ability to bind either coreceptor [116]. Viral clones with a maximum infection capability that was consistently less than 0.5% were not used.

Infectivity: Clinical observations and animal studies indicate that R5 tropic virus is better able to establish a productive infection than X4 virus [27, 36, 39, 45, 100-103]. However, the data from our *in vitro* studies seem to contradict that trend. The R5 tropic viruses consistently show lower infection levels that the X4 tropic viruses. A plausible explanation for the tropism specific differences in infectivity is the relative coreceptor availability within our target cell population. As figure 4 shows, all circulating, primary isolated, CD4+T cells express CD4 and CXCR4 while only 8.7% express measurable amounts of CCR5 coreceptors. Thus the target cell population for R5 tropic virus is much smaller than for X4. It is possible that initial infection primarily takes place in a micro environment where CCR5 coreceptors are preferentially expressed, such as the GALT [109]. But based on our studies, X4 virus and not R5 virus yields higher percent infections (%GFP) in our isolated $CD4^{+}$T cells.

An additional feature that is important to note in Figure 3 is that while the same amount of virus was used for each virus type in each donor, the y axis's scales are significantly different. With this donor to donor variability, graphs of averaged biological replicates would show identical trends but with deceptively large error bars. This issue

persists throughout all of the subsequent experiments. The magnitude of difference within Figure 2-3A is about 5 fold from highest to lowest. In Figure 2-3 B it is about 4 fold. The differences between values in A and B are also roughly 4-fold. Because the pattern is precisely the same within each $CD4^+$ T cell donor, the difference among the viral strains is attributable to biological differences in the strains and the differences between A and B can be attributed to $CD4^+$ T cell susceptibility.

Furthermore, to prevent multiplicity of infection we use virus concentrations that fall within the linear portion of the titration curve. For the R5 virus clones, this is less than 0.5% infection as measured by GFP positivity. Thus, the problem of large inter donor variability is compounded by the low levels of infection; both of these factors lead to the relatively large error bars seen in many of the figures.

Burst Size: Both a cell's activation state and the HIV-1 integration site can influence the burst size. It is possible that viruses of different tropisms preferentially infect cells with different activation states, or they may even alter the activity of the cell as they utilize their respective chemokine coreceptors. However, our experimental results show no tropism correlated trend in burst size. We do see significant variability in the burst size of each virus. Unlike the viral titrations or the suppression data, the burst size graphs have two sources of experimental variation. The low infection rates (FACS data) and the relatively low amounts of p24 produced (ELISA assay) mean that, when properly propagated, the variability is unfortunately high.

Suppression: Gag stimulated autologous $CD8^+$ T cells have previously been shown to suppress viral infection of $CD4^+$ T cells *in vitro* [117, 118]. Gag-specific $CD8^+$ T cells can target incoming virions and kill cells prior to productive infection [119, 120]. We used a suppression assay to determine if a host's cytotoxic lymphocyte (CTL) response exerts a selective pressure. In theory, the CTL response could be more effective at controlling X4 tropic virus than R5 virus. This would confirm the immune hypothesis and explain why X4 tropic virus dominates late in infection, after the immune system is severely depleted.

However, our data show no evidence of a tropism specific trend. The majority of the data was gathered using HIV^+ HAART suppressed patient cells because only $CD8^+$ T cells from HIV^+ donors will activate when exposed to gag peptides. These patient cells show low levels of infection and only moderate suppression levels (figure 6A B D E). Furthermore, proper propagation of error yields large standard deviations; this is due primarily to the low infection levels. For example, a sample can be 30% suppressed while the total difference in GFP is only 0.05%. Figures 6D and 6E illustrate this experimental limitation.

Figures 6C and 6F show a representative example of a suppression experiment using cells from an elite suppressor. These cells have two advantages: the cells are more susceptible to infection because the donor is not on HAART and elite suppressors have been shown to perform better in suppression assays [121]. Data from elite suppressor cells still shows no tropism correlated suppression trends. But here, unlike in the HIV^+ donor cells, we see enough infection and suppression to be able to recognize the consistency among the viral isolates.

Conclusion

Our data supports the hypothesis that credits replication rate and target cell availability for R5 virus's dominance and for tropism switching, respectively. Neither CTL suppression nor burst size appears to correlate with tropism, but R5 tropic virus still has some kinetic advantage. The simple viral growth modeling done here shows that, in our *in vitro* system, target cell availability is responsible for X4's higher infection rates. If early R5 virus replication primarily took place in location where it did not have a target cell disadvantage, potentially the GALT, then it would be more fit than X4 virus [109]. We conclude that R5 virus more efficiently enters its target cells, giving it a replication advantage until those target cells are depleted.

Methods

Generating Virus

Relative infectivity assays were performed with virions that had patient derived Env. We produced these viruses, which are capable of only single-round infection, as previously described [122]. Briefly, we transfected HEK293T cells with a GFP-tagged, Env-defective HIV-1 proviral vector (pNL43-ΔE-EGFP) and with a wild type patient derived HIV-1 Env expression vector. Transfections were carried out using Lipofectamine 2000 (Invitrogen, Grand Island, NY) according to the manufacture's protocol. The cells were incubated at 37ºC for 48 hours before the virus containing supernatant was layered onto a 20% sucrose buffer and ultra-centrifuged at 25,000g for 2h at 4ºC. Viral pellets were then resuspended in RPMI.

Study Subjects

Peripheral blood for the isolation of primary $CD4^+$ and $CD8^+$ T cells was obtained from HIV-1-infected patients on HAART with undetectable viral loads, from elite suppressors, and from healthy donors. All donors gave their written informed consent and the study was approved by the Institutional Review Board of Johns Hopkins University.

Single-round infectivity assay

We used a modified single-round infectivity assay to assess the effect of various Env tropism on infectivity as previously described [122, 123]. Briefly, peripheral blood mononuclear cells were obtained from healthy blood donors by Hypaque-Ficoll gradient centrifugation and then activated with phytohemagglutinin (0.5 μg/ml) and interleukin-2

(100 U/ml) for 3 days. $CD4^+$ T cells were isolated by negative selection using antibody coated magnetic beads (Miltenyi) and seeded into a 96-well plate at 1×10^5 cells per well in RPMI1640 supplemented with 10% fetal bovine serum, interleukin-2 (100 U/ml) and cytokine-rich supernatant. Cells were infected using concentrated pseudovirion preparations. To each well, 0.5-2 µl of virus was added and cells were infected by spinoculation at 1,200*g*, 30°C for 2 hours and further incubated at 37°C for 3 days [124].

After the 3 day incubation, primary $CD4^+$ T cells were washed, resuspended, and fixed with 3% formaldehyde. We quantified infectivity as the percentage of GFP^+ cells by FACS analysis (*FACS Calibur,* BD Bioscience) [122].

Quantitative FACS

QFACS was performed using standardized microbeads (QIFIKIT®*, Dako) according to the manufacturer's instructions. The primary antibodies used were purified mouse anti-human CD4, purified mouse anti-human CD184, purified mouse anti-human CD 195, and the corresponding isotype controls, all obtained from BD Biosciences. The kit consisted of a mixture of five populations of beads, each of which had a specific number of mouse monoclonal antibody (Mab) molecules per bead, and an anti-mouse FITC conjugated secondary antibody. Saturating concentrations of primary and secondary antibodies were used on the cells, and the beads were processed at the same time and in the same manner as the cells. Beads and samples were analyzed by FACS (FACS CantoII), and the data were processed using FlowJo software. This enabled us to create a standard curve relating the mean fluorescence intensity to specific antibody binding units per cell.

Suppression assay

Our suppression assay was adapted from previously described assays [125-127]. PBMCs from patients were isolated and cultured in the presence of a mixture of 129 overlapping Gag peptides (80 ng/ml for each) (NIH AIDS Reagent Program) and IL-2 (10 U/ml). Six days after stimulation, $CD8^+$ T cells were isolated by positive selection using Human CD8 Microbeads following the manufacturer's guidelines (Miltenyi Biotec).

$CD4^+$ T cells were activated and isolated as described in the Single-round infectivity assay section. They were then spinoculated in 5ml conical tubes as described [59] at 1,200 × *g, 30 ºC* for 2 h with one of the six viruses. Cells without virus were spinoculated as a negative control. After spinoclulation, $CD4^+$ T cells were washed and plated in a 96 well plate at 1×10^5 cells / well in RPMI 1640 supplemented with 10% FBS. Stimulated $CD8^+$ T cells were immediately added to the spinoculated $CD4^+$ T cells, at specified ratios. The number of $CD4^+$ T cells per well remained constant and the number of $CD8^+$ T cells was varied. Wells with only $CD4^+$ T cells (targets alone) were used as positive controls. Cells were cultured for 3 days in a final volume of 200 μL of non-stimulating media. The cells were then fixed, stained, (CD3 Pacific Blue, CD8 APC, BD) and analyzed by flow cytometry on a FACSCanto II (BD).

Figure 2-1

A

Tropism	Isolate #	
R5	10.2	4 years
R5	5-1-18	2 years
X4>R5	13.36	5 years
X4>R5	13.74	5 years
X4>>R5	13.52	5 years
X4>>R5	13.49	5 years

B

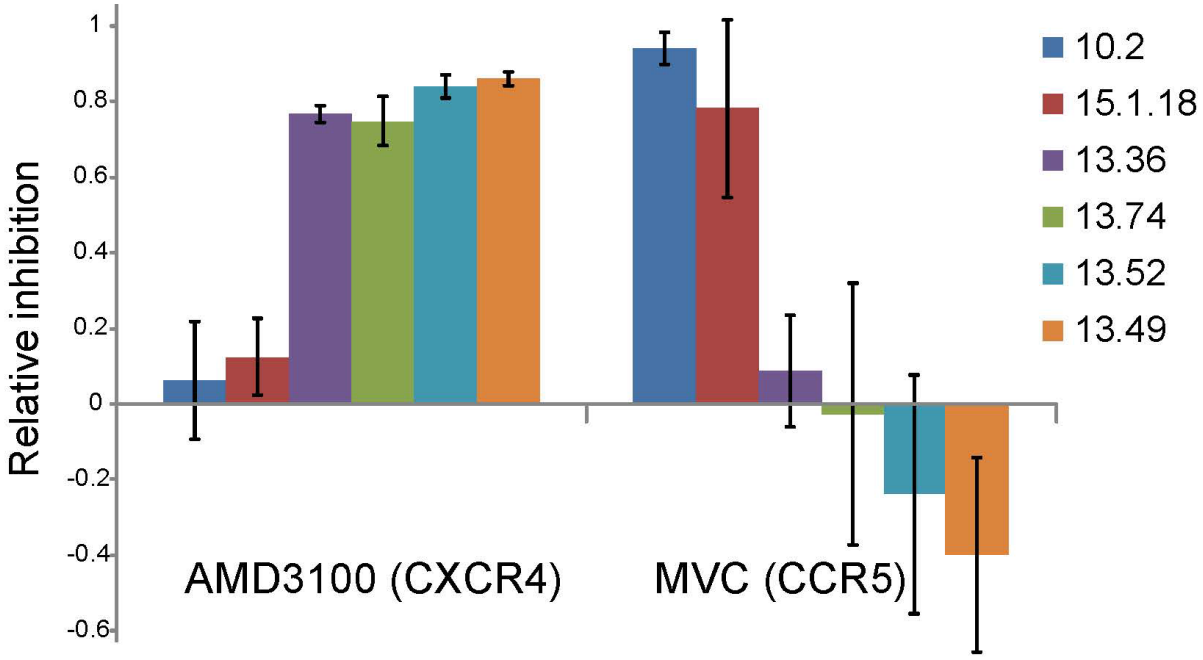

Figure 2-1 Tropisms of six patient viruses. **A**. A table listing the tropism, the isolate number and the year post initial infection that the virus was isolated. **B**. The relative inhibition of each virus caused by either the CXCR4 binding entry inhibitor AMD3100, or the CCR5 binding entry inhibitor Maraviroc (MVC).

Figure 2-2

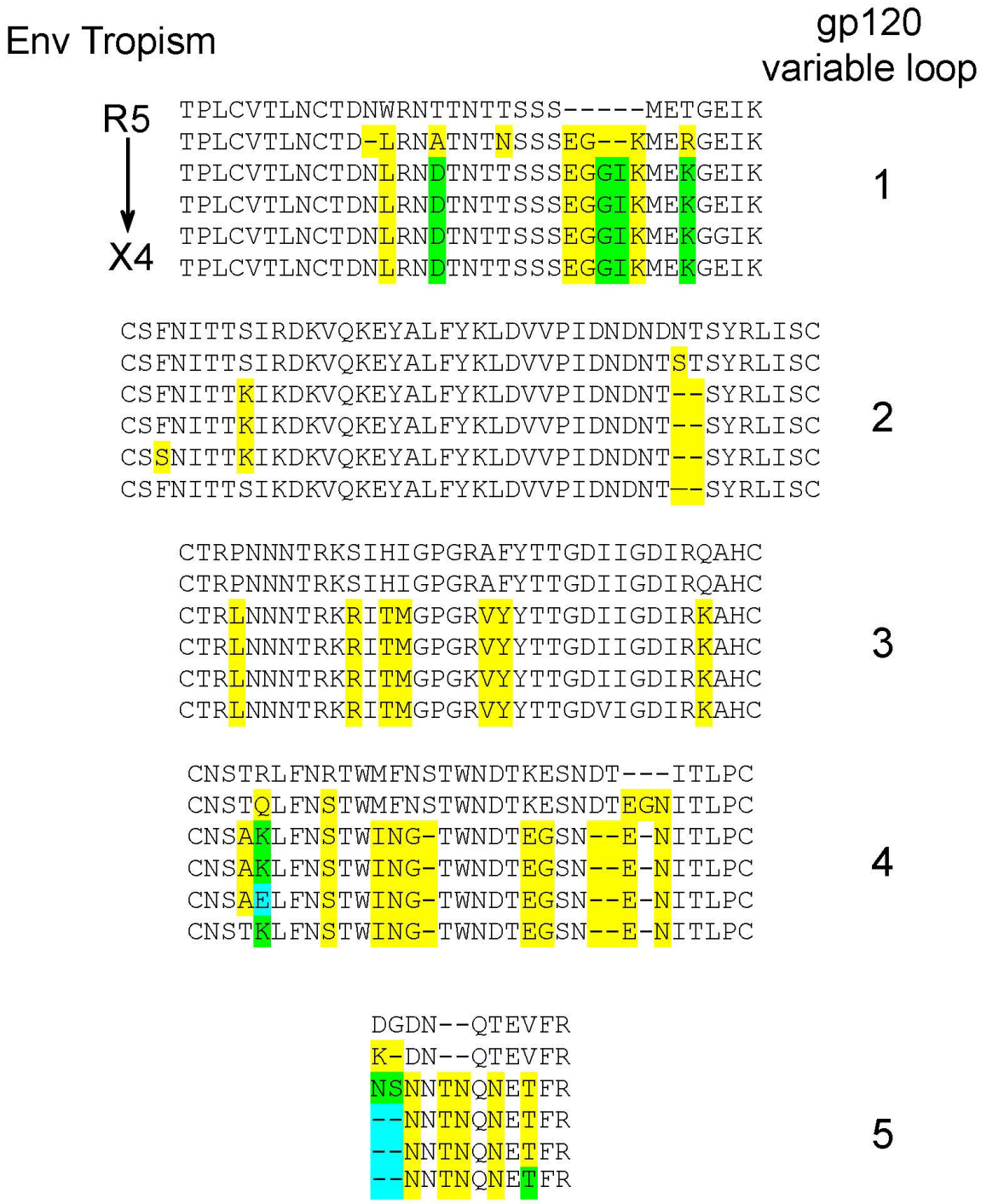
Env Tropism
gp120
variable loop
R5
X4
TPLCVTLNCTDNWRNTTNTTSSS-----METGEIK
TPLCVTLNCTD-LRNATNTNSSSEG--KMERGEIK
TPLCVTLNCTDNLRNDTNTTSSSEGGIKMEKGEIK
TPLCVTLNCTDNLRNDTNTTSSSEGGIKMEKGEIK
TPLCVTLNCTDNLRNDTNTTSSSEGGIKMEKGGIK
TPLCVTLNCTDNLRNDTNTTSSSEGGIKMEKGEIK
1
CSFNITTSIRDKVQKEYALFYKLDVVPIDNDNDNTSYRLISC
CSFNITTSIRDKVQKEYALFYKLDVVPIDNDNTSTSYRLISC
CSFNITTKIKDKVQKEYALFYKLDVVPIDNDNT--SYRLISC
CSFNITTKIKDKVQKEYALFYKLDVVPIDNDNT--SYRLISC
CSSNITTKIKDKVQKEYALFYKLDVVPIDNDNT--SYRLISC
CSFNITTSIKDKVQKEYALFYKLDVVPIDNDNT--SYRLISC
2
CTRPNNNTRKSIHIGPGRAFYTTGDIIGDIRQAHC
CTRPNNNTRKSIHIGPGRAFYTTGDIIGDIRQAHC
CTRLNNNTRKRITMGPGRVYYTTGDIIGDIRKAHC
CTRLNNNTRKRITMGPGRVYYTTGDIIGDIRKAHC
CTRLNNNTRKRITMGPGKVYYTTGDIIGDIRKAHC
CTRLNNNTRKRITMGPGRVYYTTGDVIGDIRKAHC
3
CNSTRLFNRTWMFNSTWNDTKESNDT---ITLPC
CNSTQLFNSTWMFNSTWNDTKESNDTEGNITLPC
CNSAKLFNSTWING-TWNDTEGSN--E-NITLPC
CNSAKLFNSTWING-TWNDTEGSN--E-NITLPC
CNSAELFNSTWING-TWNDTEGSN--E-NITLPC
CNSTKLFNSTWING-TWNDTEGSN--E-NITLPC
4
DGDN--QTEVFR
K-DN--QTEVFR
NSNNTNQNETFR
--NNTNQNETFR
--NNTNQNETFR
--NNTNQNETFR
5

Figure 2-2 Sequence alignments of the variable loop regions. The first sequence change is highlighted in yellow. If an amino acid changes more than once, its second change is green and the third is blue.

Figure 2-3

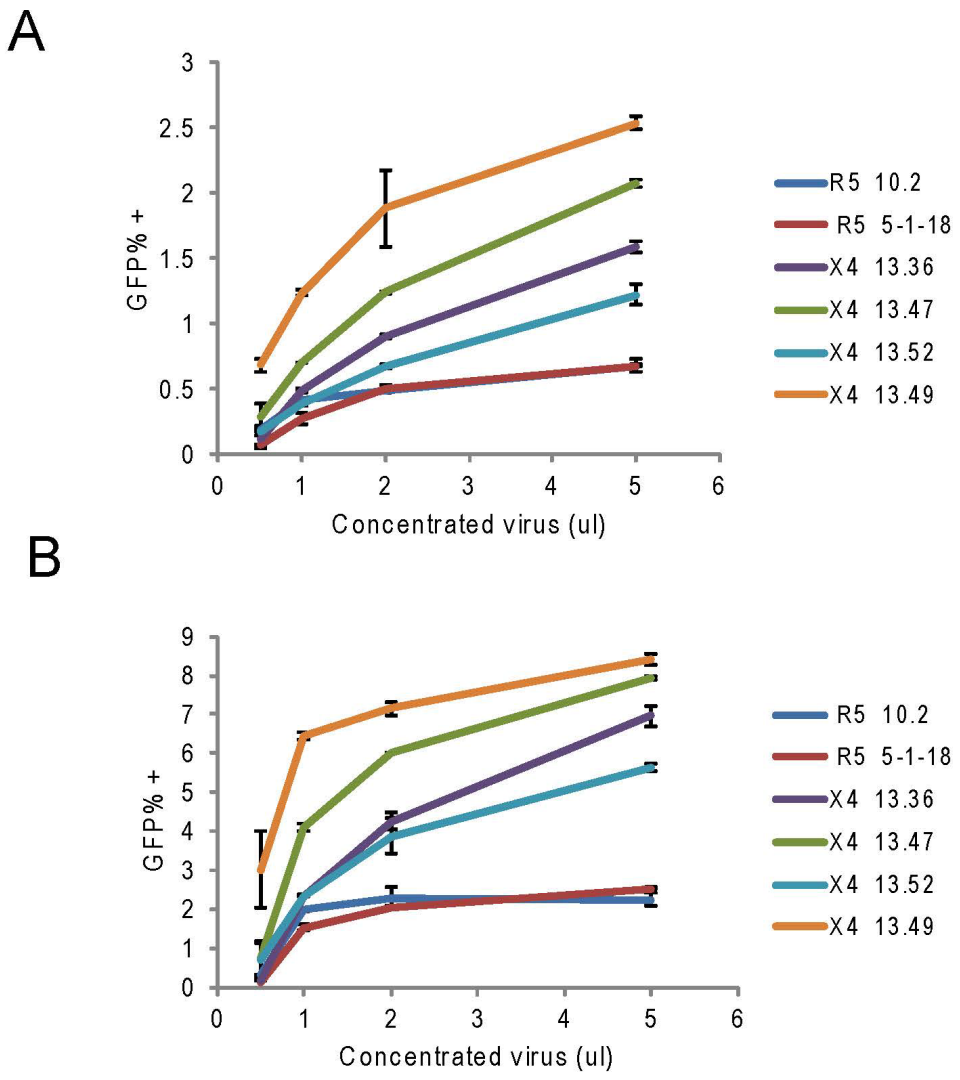

Figure 2-3 Viral titrations. Two representative donors are shown. Percent GFP^{+} (infection level) is graphed versus the volume of concentrated virus. Virus was analyzed by p24 to ensure they were at equal concentrations.

Figure 2-4

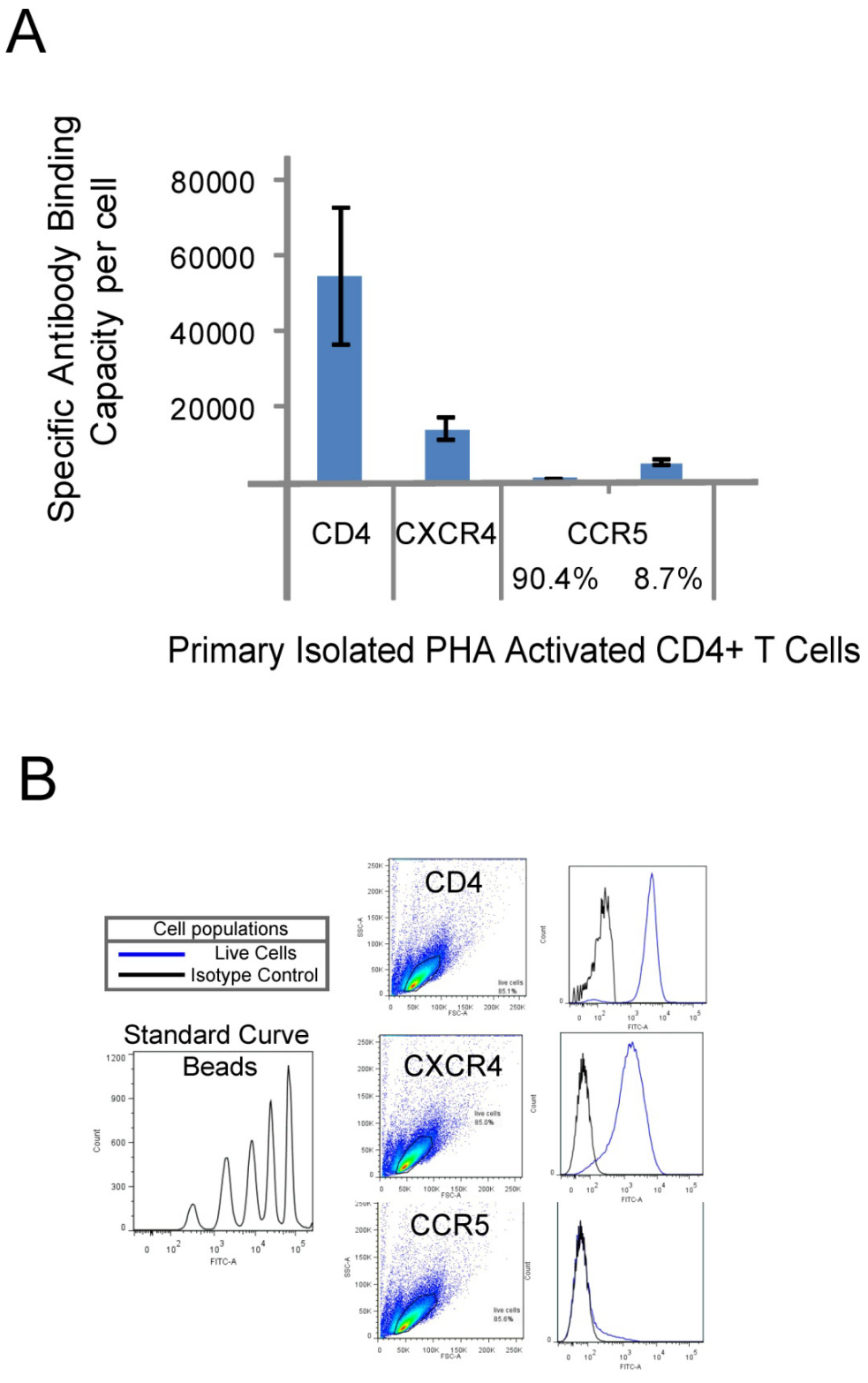
A
Specific Antibody Binding Capacity per cell
80000
60000
40000
20000
CD4
CXCR4
CCR5
90.4%
8.7%
Primary Isolated PHA Activated CD4+ T Cells
B
Cell populations
Live Cells
Isotype Control
Standard Curve
Beads
Count
FITC-A
CD4
CXCR4
CCR5
SSC-A
FSC-A
live cells
85.1%
85.0%
85.6%

Figure 2-4 Coreceptor availability. **A**. The y axis shows the specific antibody binding capacity per $CD4^+$ T cell. In this assay, one antibody binding unit corresponds to one available receptor or coreceptor. When antibodies specific for CCR5 were used, there were two distinct populations of $CD4^+$ T cells, 8.7% expressed CCR5 and 90.4% did not; numbers are an average of donors and thus don't add to 100%. **B**. Histograms of cells and of the standard curve beads are shown along with FACS plots of isolated $CD4^+$ T cells. Isotype controls are in black and specific antibody curves are in blue.

Figure 2-5

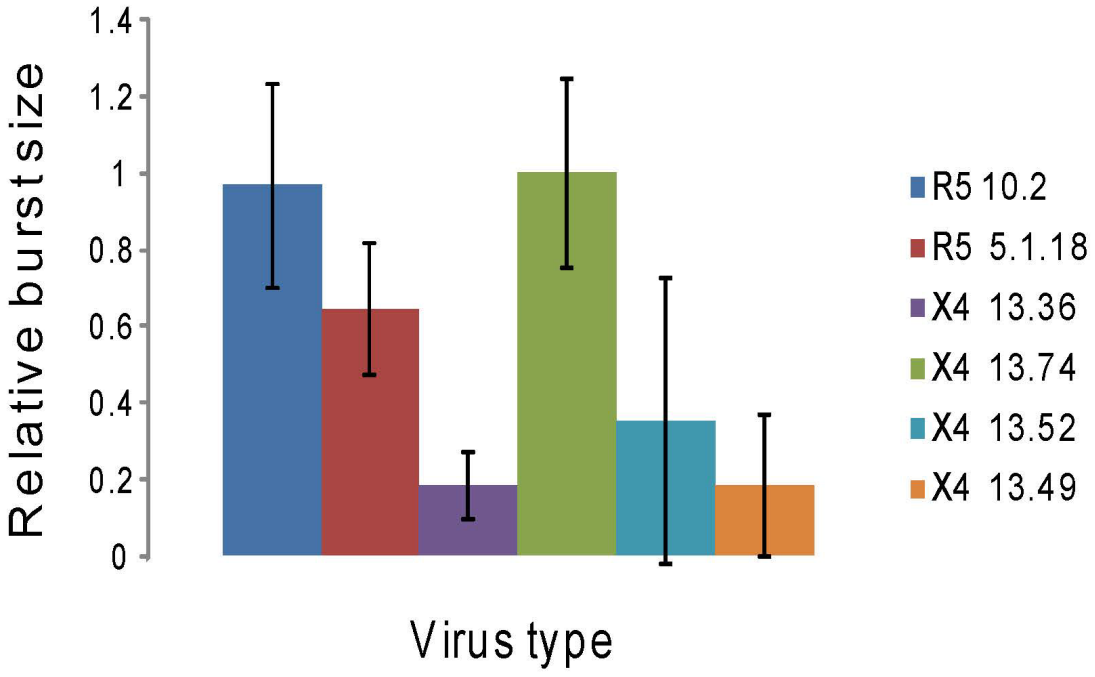

Figure 2-5 Relative burst size. Values shown are the average of five healthy donors. The y axis is the p24 present in a well three days after infection (minus day zero p24), divided by the number of cells producing virus (%GFP^+). For each donor, viral burst size was normalized, the largest virus's burst size being set to 1. Standard deviation was propagated through the calculations.

Figure 2-6

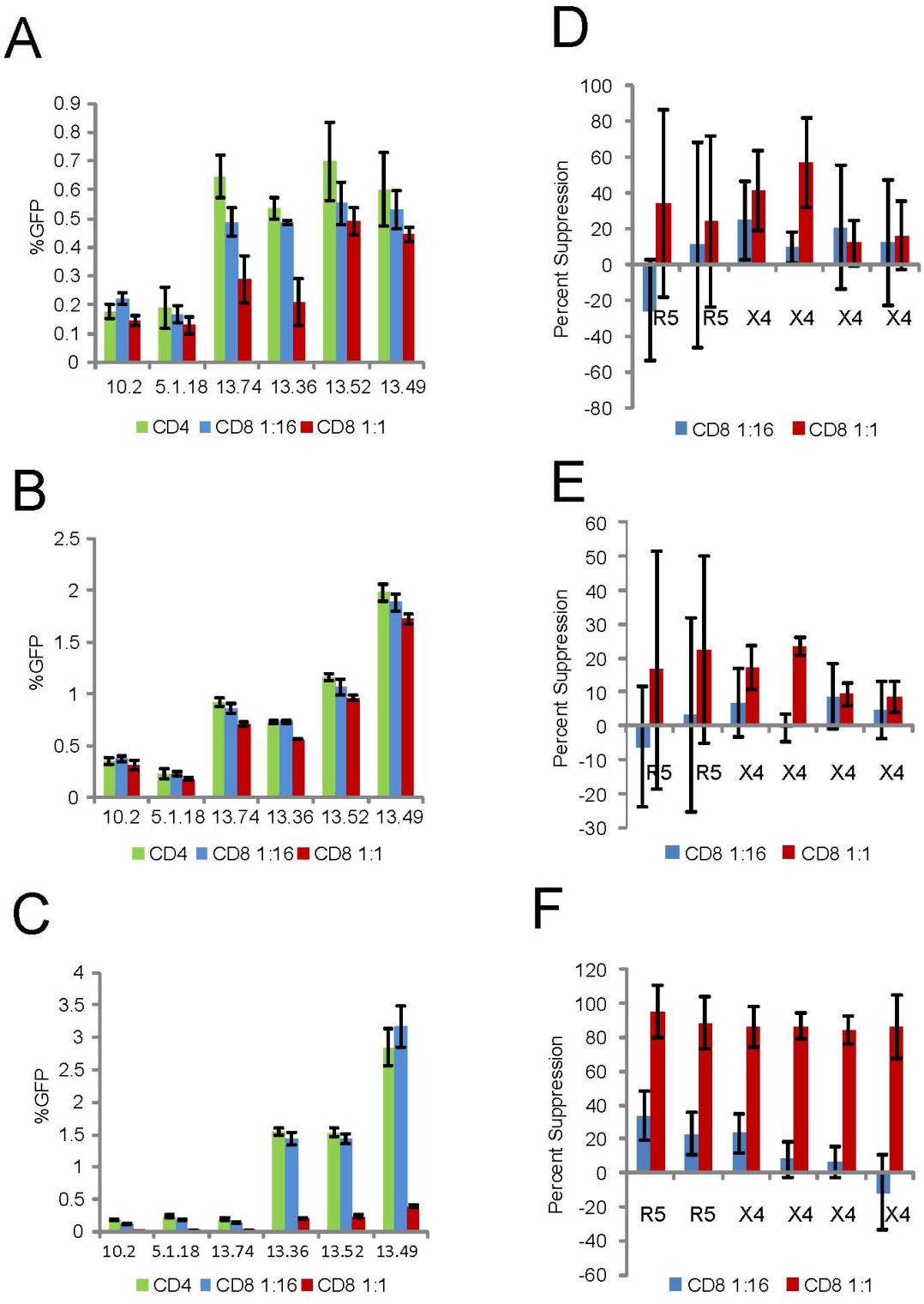
A
%GFP
0.9
0.8
0.7
0.6
0.5
0.4
0.3
0.2
0.1
0
10.2 5.1.18 13.74 13.36 13.52 13.49
CD4 CD8 1:16 CD8 1:1
B
%GFP
2.5
2
1.5
1
0.5
0
10.2 5.1.18 13.74 13.36 13.52 13.49
CD4 CD8 1:16 CD8 1:1
C
%GFP
4
3.5
3
2.5
2
1.5
1
0.5
0
10.2 5.1.18 13.74 13.36 13.52 13.49
CD4 CD8 1:16 CD8 1:1
D
Percent Suppression
100
80
60
40
20
0
-20
-40
-60
-80
R5 R5 X4 X4 X4 X4
CD8 1:16 CD8 1:1
E
Percent Suppression
60
50
40
30
20
10
0
-10
-20
-30
R5 R5 X4 X4 X4 X4
CD8 1:16 CD8 1:1
F
Percent Suppression
120
100
80
60
40
20
0
-20
-40
-60
R5 R5 X4 X4 X4 X4
CD8 1:16 CD8 1:1

Figure 2-6 Suppression assays. Three donors are shown, A/D and B/E are HAART patients and C/F is an elite suppressor. Green is the control result from wells containing only CD4+ T cells. Blue represents wells with a 1:16 ratio of $CD8^+$ T:$CD4^+$T cells. For the red bars the ratio is 1:1. A-C show $CD4^+$ T cell infection levels for each virus. D-F shows the calculated percent suppression. Standard deviation is propagated through the calculation.

Supplemental Table 2-1

Donor A	10.2 R5	1-5-18 R5	13.36 X4	13.48 X4	13.52 X4	13.49 X4
5.0 µl	0.681	0.681	1.589	1.219	2.074	2.538
2.0 µl	0.488	0.510	0.908	0.673	1.241	1.887
1.0 µl	0.412	0.272	0.488	0.392	0.702	1.234
0.5 µl	0.187	0.071	0.115	0.176	0.288	0.682

Donor B	10.2 R5	1-5-18 R5	13.36 X4	13.48 X4	13.52 X4	13.49 X4
5.0 µl	2.246	2.537	6.948	5.626	7.928	8.415
2.0 µl	2.259	2.046	4.259	3.875	6.009	7.145
1.0 µl	1.971	1.523	2.338	2.343	4.094	6.428
0.5 µl	0.297	0.121	0.192	0.676	0.742	3.004

Supplemental Table 2-1 Infection data (%GFP) corresponding to Figure 2-3. The %GFP values graphed in Figure 2-3 and used in kinetic rate constant (*k*) calculations.

Chapter 3:

Conclusions and perspectives

Overall, this work provides evidence against many of the proposed causes for X4 and R5 virus's phenotypic differences, but the positive data it produces is vague. R5 virus replication does have some kinetic advantage over X4 virus, but this advantage does not come from the entry machinery or from the viral burst size. Some other unidentified factor, potentially cellular activation, must be responsible.

Chapter one confirms that HIV-1 entry requires only one or two functional Env entry spikes. It also concludes that an individual virion, on average, has between one and three spikes on its surface that are both functional and able to simultaneously contact a target cell. However, this in depth analysis of the viral entry process failed to find a significant biophysical difference between HXB2 (X4 tropic) and Yu2 (R5 tropic) viruses. Both tropisms tested appear to have indistinguishable entry stoichiometry.

Chapter two provides evidence against CTL suppression or burst size playing a role in early R5 dominance. The viral growth modeling shows that, in our *in vitro* system, target cell availability is responsible for X4's higher infection rates. But this does not necessarily correlate to early infection *in vivo*. The most interesting difference between the two tropisms discovered here is the infection rate constant; this number comes from equation 2 which includes factors for infection rate, burst size and, target cell availability. Based on this equation and the data experimentally collected in chapter two, R5 virus has a more than two fold replication advantage over some of the X4 viral isolates. If the difference in target cell availability during early infection turns out not to overwhelmingly favor X4 growth, this kinetic difference could explain R5's initial dominance. In later infection, it possible that the tropism switch is a result of random chance or is influenced by changing cellular target populations.

Overall, our data supports the hypothesis that credits replication rate and target cell availability for R5 virus's dominance and for tropism switching, respectively. We conclude that R5 virus more efficiently causes infection in its target cells and this gives it a replication advantage until those target cells are depleted.

References

1. UNAIDS: **Report on the global AIDS epidemic.** 2013

2. Perelson AS, Neumann AU, Markowitz M, Leonard JM, Ho DD: **HIV-1 dynamics in vivo: virion clearance rate, infected cell life-span, and viral generation time**. *Science* 1996, **271**:1582–1586.

3. Gallo SA, Finnegan CM, Viard M, Raviv Y, Dimitrov A, Rawat SS, Puri A, Durell S, Blumenthal R: **The HIV Env-mediated fusion reaction**. *Biochim. Biophys. Acta* 2003,**1614**:36–50.

4. Robey W, Safai B, Oroszlan S, Arthur L, Gonda M, et al.: **Characterization of envelope and core structural gene-products of HTLV-III with sera from AIDS patients**. *Science* 1985, **228**: 593–595.

5. Veronese F, Devico A, Copeland T, Oroszlan S, Gallo R, et al.: **Characterization of gp41 as the transmembrane protein coded by the HTLV- III/LAV envelope gene**. *Science* 1985, **229**: 1402–1405.

6. Wyatt R, Sodroski J: **The HIV-1 envelope glycoproteins: fusogens, antigens, and immunogens**. *Science* 1998, **280**: 1884–1888.

7. Shang-Rung Wu, Löving R, Lindqvist B, Hebert H, Koeck, PJB, Sjöberg M, Garoff H: **Single-particle cryoelectron microscopy analysis reveals the HIV-1 spike as a tripod structure**. *PNAS* 2010, **107**(44):18844-18849.

8. Roux KH, Taylor KA: **AIDS virus envelope spike structure.** *Current Opinion in Structural Biology* 2007, **17**:244-252.

9. Eckert DM, PS Kim: **Mechanisms of viral membrane fusion and its inhibition.** *Annu. Rev. Biochem*. 2001, **70**:777–810.

10. Wyatt R, Kwong PD, Desjardins E: **The antigenic structure of the HIV gp120 envelope glycoprotein.** *Nature* 1998, **6686**:705-711.

11. Klatzmann D, Champagne E, Chamaret S, Gruest J, Guetard D, et al.: **T- lymphocyte T4 molecule behaves as the receptor for human retrovirus LAV.** *Nature* 1984, **312**: 767–768.

12. McDougal J, Kennedy M, Sligh J, Cort S, Mawle A, et al: **Binding of HTLV-III/LAV to T4+ T-cells by a complex of the 110K viral protein and the T4 molecule**. *Science* 1986, 231: 382–385.

13. Dalgleish AG, Beverley PC. Clapham PRD, Crawford H, Greaves MF, Weiss RA: **The CD4 (T4) antigen is an essential component of the receptor for the AIDS retrovirus**. *Nature* 1984, **312**:763–767.

14. LaBranche CC, Galasso G, Moore JP, Bolognesi DP, Hirsch MS, Hammer SM: **HIV fusion and its inhibition.** *Antiviral research* 2001, **50**:95-115

15. Kwong PD, Wyatt R, Robinson J, Sweet RW, Sodroski J, Hendrickson WA: **Structure of an HIV gp120 envelope glycoprotein in complex with the CD4 receptor and a neutralizing human antibody**. *Nature* 1998, **393**: 648-59

16. Alkhatib G, Combadiere C, Broder CC, Feng Y, Kennedy PE, Murphy PM, Berger EA: **CC CKR5: a RANTES, MIP-1alpha, MIP-1beta receptor as a fusion cofactor for macrophage-tropic HIV-1**. *Science* 1996, **272**:1955–1958.

17. Bleul CC, Farzan M, Choe H, Parolin C, Clark-Lewis I, Sodroski J, Springer TA:. **The lymphocyte chemoattractant SDF-1 is a ligand for LESTR/fusin and blocks HIV-1 entry**. *Nature* 1996, **382**:829–833.

18. Choe H, Farzan M, Sun Y, Sullivan N, Rollins B, Ponath PD, Wu L, Mackay CR, LaRosa G, Newman W, Gerard N, Gerard C, Sodroski J: **The beta-chemokine receptors CCR3 and CCR5 facilitate infection by primary HIV-1 isolates**. *Cell* 1996, **85**:1135–1148.

19. Deng H, Liu R, Ellmeier W, Choe S, Unutmaz D, Burkhart M, Di Marzio P, Marmon S, Sutton RE, Hill CM, Davis CB, Peiper SC, Schall TJ, Littman DR, Landau N: **Identification of a major co-receptor for primary isolates of HIV-1.** *Nature* 1996, **381**:661–666.

20. Doranz BJ, Rucker J, Yi Y, Smyth RJ, Samson M, Peiper SC, Parmentier M, Collman RG, Doms RW: **A dual-tropic primary HIV-1 isolate that uses fusin and the beta-chemokine receptors CKR-5, CKR-3, and CKR-2b as fusion cofactors.** *Cell* 1996, **85**:1149–1158.

21. Feng Y, Broder CC, Kennedy PE, Berger EA: **HIV-1 entry cofactor: functional cDNA cloning of a seven-transmembrane, G protein- coupled receptor**. *Science* 1996, **272**:872–877.

22. Oberlin E, Amara A, Bachelerie F, Bessia C, Virelizier JL, Arenzana- Seisdedos F, Schwartz O, Heard JM, Clark-Lewis I, Legler DF, Loetscher M, Baggiolini M, Moser B: **The CXC chemokine SDF-1 is the ligand for LESTR/fusin and prevents infection by T-cell-line-adapted HIV-1.** *Nature* 1996, **382**:833–835.

23. Sattentau Q, Moore J: **Conformational-changes induced in the human-immunodeficiency-virus envelope glycoprotein by soluble cd4 binding**. *Journal of experimental medicine* 1991, **174**: 407–415.

24. Liu J, Bartesaghi A, Borgnia MJ, Sapiro G, Subramaniam S: **Molecular architecture of native HIV-1 gp120 trimers**. *Nature* 2008, **455**:109-113

25. Alkhatib G: **The biology of CCR5 and CXCR4**. *Curr Opin HIV AIDS*. 2009, **4**:96-103.

26. Moore JP, Trkola A, Dragic T: **Co-receptors for HIV-1 entry**. *Current opinion in immunology* 1997, **9**:551-562.

27. Moore JP, Kitchen SG, Pugach P, Zack JA: **Understanding the transmission and pathogenesis of human immunodeficiency virus type 1 infection.** *Aids Research and Human Retroviruses* 2004, **20**:111-126.

28. Berger EA: **A new classification for HIV-1.** *Nature* 1988, **17**:657-700.

29. Raymond S, Delobel P, Mavigner M, Cazabat M, Souyris C, et al.: **Correlation between genotypic predictions based on V3 sequences and phenotypic determination of HIV-1 tropism.** *AIDS* 2008, **22**: F11–F16.

30. Chesebro B, Nishio J, Perryman S, Cann A, O'Brien W, Chen IS, Wehrly K: **Identification of human immunodeficiency virus envelope gene sequences influencing viral entry into CD4-positive HeLa cells, T-leukemia cells, and macrophages**. *J Virol*. 1991, **65**:5782-5789.

31. Groenink M, Fouchier RA, Broersen S, Baker CH, Koot M, van't Wout AB, Huisman HG, Miedema F, Tersmette M, Schuitemaker H: **Relation of phenotype evolution of HIV-1 to envelope V2 configuration**. *Science* 1993, **260**:1513-1516.

32. O'Brien WA, Koyanagi Y, Namazie A, Zhao JQ, Diagne A, Idler K, Zack JA, Chen IS: **HIV-1 tropism for mononuclear phagocytes can be determined by regions of gp120 outside the CD4-binding domain.** *Nature* 1990, **348**:69-73.

33. Shioda T, Levy JA, Cheng-Mayer C: **Small amino acid changes in the V3 hypervariable region of gp120 can affect the T-cell-line and macrophage tropism of human immunodeficiency virus type 1**. *Proc Natl Acad Sci USA.* 1992, **89**:9434-9438.

34. De Jong JJ, De Ronde A, Keulen W, Tersmette M, Goudsmit J: **Minimal requirements for the human immunodeficiency virus type 1 V3 domain to support the syncytium- inducing phenotype: analysis by single amino acid substitution**. *J Virol.* 1992, **66**:6777-6780.

35. Fouchier RA, Groenink M, Kootstra NA, Tersmette M, Huisman HG, Miedema F, Schuitemaker H: **Phenotype-associated sequence variation in the third variable domain of the human immunodeficiency virus type 1 gp120 molecule.** *J Virol*. 1992, **66**:3183-3187.

36. Keele BF, Giorgi EE, Salazar-Gonzalez JF, Decker JM, Pham KT, Salazar MG, Sun C, Grayson T, Wang S, Li H, Wei X, Jiang C, Kirchherr JL, Gao F, Anderson JA,

Ping L, Swanstrom R, Tomaras GD, Blattner WA, Goepfert PA, Kilby JM, Saag MS, Delwart EL, Busch MP, Cohen MS, Montefiori DC, Haynes BF, Gaschen B, Athreya GS, Lee HY, Wood N, Seoighe C, Perelson AS, Bhattacharya T, Korber BT, Hahn BH, Shaw GM: **Identification and characterization of transmitted and early founder virus envelopes in primary HIV-1 infection**. *Proc Natl Acad Sci. USA*. 2008, **105**:7552-7557.

37. Salazar-Gonzalez JF, Bailes E, Pham KT, Salazar MG, Guffey MB, Keele BF. Derdeyn CA. Farmer P. Hunter E. Allen S. Manigart O. Mulenga J. Anderson J. A. Swanstrom R., Haynes B. F., Athreya G. S., Korber B. T. M., Sharp P. M., George M. Shaw GM. Beatrice H. Hahn BH: **Deciphering human immunodeficiency virus type 1 transmission and early envelope diversification by single-genome amplification and sequencing.** *J Virol*. 2008, **82:**3952-3970.

38. Long EM, Rainwater SM, Lavreys L, Mandaliya K, Overbaugh J: **HIV type 1 variants transmitted to women in Kenya require the CCR5 coreceptor for entry, regardless of the genetic complexity of the infecting virus.** *AIDS Res Hum Retroviruses* 2002, **18**:567-576.

39. van't Wout AB, Kootstra NA, Mulder-Kampinga GA, Albrecht van Lent N, Scherpbier HJ, Veenstra J, Boer K, Coutinho RA, Miedema F, Schuitemaker H: **Macrophage-tropic variants initiate human immunodeficiency virus type 1 infection after sexual, parenteral, and vertical transmission**. *J Clin Invest*. 1994, **94**:2060-2067.

40. Zhu T, Mo H, Wang N, Nam DS, Cao Y, Koup RA, Ho DD: **Genotypic and phenotypic characterization of HIV-1 patients with primary infection.** *Science*. 1993, **261**:1179-1181.

41. Schuitemaker H, van't Wout AB, Lusso P: **Clinical significance of HIV-1 coreceptor usage.** *Journal of Translational Medicine* 2010, **9**(Suppl 1):S5

42. Keele BF, Giorgi EE, Salazar-Gonzalez JF, Decker JM, Pham KT, et al.: **Identification and characterization of transmitted and early founder virus envelopes in primary HIV-1 infection**. *Proc Natl Acad Sci U S A.* 2008, **105**:7552-7557

43. Harouse JM, Buckner C, Gettie A, Fuller R, Bohm R, Blanchard J, Cheng-Mayer C: **CD8 T cell-mediated CXC chemokine receptor 4-simian/human immunodeficiency virus suppression in dually infected rhesus macaques.** *Proc Natl Acad Sci U S A.* 2003, **100**(19):10977-82.

44. Cornelissen M, Mulder-Kampinga G, Veenstra J, Zorgdrager F, Kuiken C, Hartman S, Dekker J, van der Hoek L, Sol C, Coutinho R: **Sycytium-inducing (SI) phenotype suppression at seroconversion after intramuscular inoculation of a non-syncytium-inducing/SI phenotypically mixed human immunodeficiency virus population.** *J Virol*. 1995, **69**(3):1810-8.

45. Pratt RD, Shapiro JF, McKinney N, Kwok S, Spector SA: **Virologic characterization of primary human-immunodeficiency-virus type-1 infection in a health-care worker following needle stick injury**. *J Infect Dis.* 1995, **172** (3): 851-854.

46. Glushakova S, Yi Y, Grivel JC, Singh A, Schols D, Clercq ED, Collman RG, Leonid Margolis L: **Preferential coreceptor utilization and cytopathicity by dual-tropic HIV-1 in human lymphoid tissue ex vivo** *J Clin Invest*. 1999, **104**(5): R7–R11.

47. Koot M, Keet IP, Vos AH, de Goede RE, Roos MT, Coutinho RA, Miedema F, Schellekens PT, Tersmette M: **Prognostic value of HIV-1 syncytium-inducing phenotype for rate of CD4+ cell depletion and progression to AIDS.** *Ann Intern Med.* 1993, **118**:681-8.

48. Rowland-Jones SL: **Timeline: AIDS pathogenesis: what have two decades of HIV research taught us?** *Nat Rev Immunol*. 2003, **3**:343-8.

49. Grivel JC, Margolis LB: **CCR5 and CXCR4-tropic HIV-1 are equally cytopathic for their T-cell targets in human lymphoid tissue.** *Nature Medicine* 1999, **5**:344-346

50 Salzwedel K, Berger EA: **Cooperative subunit interactions within the oligomeric envelope glycoprotein of HIV-1: functional comple- mentation of specific defects in gp120 and gp41.** *Proc. Natl. Acad. Sci. USA* 2000, **97**:12794–12799.

51. Magnus C, Rusert P, Bonhoeffer S, Trkola A, Regoes RR: **Estimating the stoichiometry of human immunodeficiency virus entry**. *J Virol* 2009, **83**:1523-1531.

52. Borrow P, Lewicki H, Wei X, Horwitz MS, Peffer N, Meyers H, Nelson JA, Gairin JE, Hahn BH, Oldstone MB, Shaw GM: **Antiviral pressure exerted by HIV-1-specific cytotoxic T lymphocytes (CTLs) during primary infection demonstrated by rapid selection of CTL escape virus**. *Nat. Med.* 1997, **3**:205–211.

53. Walker BD, Chakrabarti S, Moss B, Paradis TJ, Flynn T, Durno AG, Blumberg RS, Kaplan JC, Hirsch MS, Schooley RT**: HIV-specific cytotoxic T lymphocytes in seropositive individuals.** *Nature* 1987, **328**:345–348.

54. Koup RA, Safrit JT, Cao Y, Andrews CA, McLeod G, Borkowsky W, Farthing C, Ho DD: **Temporal association of cellular immune responses with the initial control of viremia in primary human immunodeficiency virus type 1 syndrome.** *J. Virol.* 1994, **68**:4650–4655

55. Gandhi RT, Walker BD: **Immunologic control of HIV-1** *Annu. Rev. Med.* 2002, **53**:149–172

56. Hersperger AR, Migueles SA, Betts MR, Connors M: **Qualitative features of the HIV-specific CD8+ T-cell response associated with immunologic control** *Curr. Opin. HIV AIDS* 2011, **6**:169–173

57. Schmitz JE, Kuroda MJ, Santra S, Sasseville VG, Simon MA, Lifton MA, Racz P, Tenner-Racz K, Dalesandro M, Scallon BJ: **Control of viremia in simian immunodeficiency virus infection by CD8+ lymphocytes**. *Science* 1999, **283**:857–860

58. Regoes RR, Bonhoeffer S, **The HIV coreceptor switch: a population dynamical perspective.** *Trends Microbiol*. 2005, **6**:269-77.

59. Miedema F, Tersmette M, van Lier RAW: **AIDS pathogenesis: a dynamic interaction between HIV and the immune system.** *Immunol. Today* 1990, **11**:293-297

60. Schellekens PT, Roos MT, De Wolf F, Lange JM, Miedema F: **Low T cell responsiveness to activation via CD3/TCR is a prognostic marker for acquired-immunodeficiency-syndrome (AIDS) in human immunodeficiency virus-1 (HIV-1) infected men**. *J Clin. Immunol.* 1990 **10**:121-127

61. LaBranche CC, Galasso G, Moore JP, Bolognesi DP, Hirsch MS, Hammer SM: **HIV fusion and its inhibition.** *Antiviral research* 2001, **50:**95-115.

62. Wilen CB, Tilton JC, Doms RW**: Molecular mechanisms of HIV entry.** *Adv Exp Med Biol* 2012, **726**:223-42.

63. Alkhatib G: **The biology of CCR5 and CXCR4**. *Curr Opin HIV AIDS* 2009, **4**:96-103.

64. Wyatt R, Sodroski J: **The HIV-1 envelope glycoproteins: Fusogens, antigens, and immunogens.** *Science* 1998, **280**: 1884–1888.

65. Zhang H, Zhou Y, Alcock C, Kiefer T, Monie D, Siliciano J, Li Q, Pham P, Cofrancesco J, Persaud D, Siliciano RF: **Novel single-cell–level phenotypic assay for residual drug susceptibility and reduced replication capacity of drug-resistant human immunodeficiency virus type 1**. *J Virol* 2004, **78**:1718-1729.

66. Babcock GJ, Mirzabekov T, Wojtowicz W, Sodroski J: **Ligand binding characteristics of CXCR4 incorporated into paramagnetic proteoliposomes.** *J Biol Chem* 2001, **276**:38433.

67. Hoffman TL, Canziani G, Jia L, Rucker J, Doms RW: **A biosensor assay for studying ligand-membrane receptor interactions: Binding of antibodies and HIV-1 Env to chemokine receptors**. *Proc Natl Acad Sci USA* 2000, **97**:11215.

68. Wu L, Gerard NP, Wyatt R, Choe H, Parolin C, Ruffing N, Borsetti A, Cardoso AA, Desjardin E, Newman W, Gerard C, Sodroski J: **CD4-induced interaction of**

primary HIV-1 gp120 glycoproteins with the chemokine receptor CCR-5. *Nature* 1996, **384**:179-183.

69. Doranz BJ, Baik SSW, Doms RW: **Use of a gp120 binding assay to dissect the requirements and kinetics of human immunodeficiency virus fusion events**. *J Virol* 1999, **73**:10346-10358.

70. Lee B, Sharron M, Montaner LJ, Weissman D, Doms RW: **Quantification of CD4, CCR5, and CXCR4 levels on lymphocyte subsets, dendritic cells, and differentially conditioned monocyte-derived macrophages**. *Proc Natl Acad Sci USA*. 1999, **96**:5215-5220.

71. Sougrat R, Bartesaghi A, Lifson JD, Bennett AE, Bess JW, Zabransky DJ, Subramaniam S: **Electron tomography of the contact between T cells and SIV/HIV-1: Implications for viral entry.** *PLoS Pathog* 2007, **4**;3(5):e63.

72. Magnus C, Regoes RR: **Estimating the Stoichiometry of HIV Neutralization**. *PLoS Comput Biol* 2010, **6**(3):e1000713.

73. Klasse PJ: **Modeling how many envelope glycoprotein trimers per virion participate in human immunodeficiency virus infectivity and its neutralization by antibody**. *J Virol* 2007, **369**:245-262.

74. Herrera C, Klasse PJ, Kibler CW, Michael E, Moore JP, Beddows S: **Dominant-negative effect of hetero-oligomerization on the function of the human immunodeficiency virus type 1 envelope glycoprotein complex.** *J Virol* 2006, **351**:121-132.

75. Yang X, Kurteva S, Ren X, Lee S, Sodroski J: **Subunit stoichiometry of human immunodeficiency virus type 1 envelope glycoprotein trimers during virus entry into host cells.** *J Virol* 2006, **80**:4388-95.

76. Yang X, Kurteva S, Lee S, Sodroski J: **Stoichiometry of antibody neutralization of human immunodeficiency virus type 1**. *J Virol* 2005, **79**:3500-3508.

77. Yang X, Kurteva S, Ren X, Yang SL, Sodroski J: **Stoichiometry of envelope glycoprotein trimers in the entry of Human Immunodeficiency Virus type 1**. *J Virol* 2005, **79**:12132-47.

78. Schønning K, Lund O, Søgaard Lund O, Hansen JE: **Stoichiometry of monoclonal antibody neutralization of T-cell line-adapted human immunodeficiency virus type 1.** *J Virol* 1999, **73**: 8364-8370.

79. Kuhmann SE, Platt EJ, Kozak SL, Kabat D: **Cooperation of multiple CCR5 coreceptors is required for infections by human immunodeficiency virus type 1**. *J Virol* 2000, **75**(15):7005-7015.

80. Salzwedel K, Berger EA: **Complementation of diverse HIV-1 Env defects through cooperative subunit interactions: a general property of the functional trimer**. *Retrovirology* 2009, **6**:75.

81. Zarr MA (2014): **Relative infectivity data set for figures 3 and 4**. *LabArchives*. http://dx.doi.org/10.6070/H4C53HS7

82. Kellam P, Larder BA: **Recombinant virus assay: a rapid, phenotypic assay for assessment of drug susceptibility of human immunodeficiency virus type 1 isolates.** *Antimicrob Agents Chemother* 1994, **38**:23-30.

83. Sagar M, Kirkegaard E, Long EM, Celum C, Buchbinder S, Daar ES, Overbaugh J: **Human immunodeficiency virus type 1 (HIV-1) diversity at time of infection is not restricted to certain risk groups or specific HIV-1 subtypes.** *J Virol.* 2004 **78**(13):7279-83.

84 Wolinsky SM, Wike CM, Korber BT, Hutto C, Parks WP, Rosenblum LL, Kunstman KJ, Furtado MR, Muñoz JL: **Selective transmission of human immunodeficiency virus type-1 variants from mothers to infants**. *Science*. 1992, **255**(5048):1134-7.

85 Zhang LQ, MacKenzie P, Cleland A, Holmes EC, Brown AJ, Simmonds P: **Selection for specific sequences in the external envelope protein of human immunodeficiency virus type 1 upon primary infection.** *J Virol*. 1993, **67**(6):3345-56.

86. Shankarappa R, Margolick JB, Gange SJ, Rodrigo AG, Upchurch D, Farzadegan H, Gupta P, Rinaldo CR, Learn GH, He X, Huang XL, Mullins JI: **Consistent viral evolutionary changes associated with the progression of human immunodeficiency virus type 1 infection**. *J Virol*. 1999, **73**(12):10489-502.

87. Mansky LM, Temin HM: **Lower in vivo mutation rate of human immunodeficiency virus type 1 than that predicted from the fidelity of purified reverse transcriptase.** *J Virol*. 1995, **69**(8):5087-94.

88. Shriner D, Rodrigo AG, Nickle DC, Mullins JI: **Pervasive genomic recombination of HIV-1 in vivo.** *Genetics* 2004, **167**(4):1573-83.

89. Brumme ZL, Goodrich J, Mayer HB, Brumme CJ, Henrick BM, Wynhoven B, Asselin JJ, Cheung PK, Hogg RS, Montaner JS, Harrigan PR: **Molecular and clinical epidemiology of CXCR4-using HIV-1 in a large population of antiretroviral-naive individuals**. *J Infect Dis*. 2005, **192**(3):466-74.

90. Moyle GJ, Wildfire A, Mandalia S, Mayer H, Goodrich J, Whitcomb J, Gazzard BG: **Epidemiology and predictive factors for chemokine receptor use in HIV-1 infection.** *J Infect Dis*. 2005, **191**(6):866-72.

91. Schuitemaker H, Koot M, Kootstra NA, Dercksen MW, de Goede RE, van Steenwijk RP, Lange JM, Schattenkerk JK, Miedema F, Tersmette M: **Biological phenotype of human immunodeficiency virus type 1 clones at different stages of infection:**

progression of disease is associated with a shift from monocytotropic to T-cell-tropic virus population. *J. Virol*. 1992, **66**:1354–1360.

92. van Rij RP, Blaak H, Visser JA, Brouwer M, Rientsma R, Broersen S, de Roda Husman AM, Schuitemaker H: **Differential coreceptor expression allows for independent evolution of non-syncytium-inducing and syncytium-inducing HIV-1.** *J Clin Invest.* 2000, **106**(8):1039-52.

93. Wilkin TJ, Su Z, Kuritzkes DR, Hughes M, Flexner C, Gross R, Coakley E, Greaves W, Godfrey C, Skolnik PR, Timpone J, Rodriguez B, Gulick RM: **HIV type 1 chemokine coreceptor use among antiretroviral-experienced patients screened for a clinical trial of a CCR5 inhibitor: AIDS Clinical Trial Group A5211.***Clin Infect Dis.* 2007, **44**(4):591-5.

94. Bozzette SA, McCutchan JA, Spector SA, Wright B, Richman DD: **A cross-sectional comparison of persons with syncytium- and non-syncytium-inducing human immunodeficiency virus.** *J Infect Dis*. 1993, **168**(6):1374-9.

95. Connor RI, Mohri H, Cao Y, Ho DD: **Increased viral burden and cytopathicity correlate temporally with CD4+ T-lymphocyte decline and clinical progression in human immunodeficiency virus type 1-infected individuals.** *J Virol*. 199, **67**(4):1772-7.

96. Koot M, van 't Wout AB, Kootstra NA, de Goede RE, Tersmette M, Schuitemaker H: **Relation between changes in cellular load, evolution of viral phenotype, and the clonal composition of virus populations in the course of human immunodeficiency virus type 1 infection.** *J Infect Dis.* 1996, **173**(2):349-54.

97. Koot M, Keet I, Vos A, deGoede R, Roos M, Coutinho R, Miedema F, Schellekens P, Tersmette M: **Prognostic value of HIV-1 syncytium-inducing phenotype for rate of CD4+ cell depletion and progression to AIDS**. *Ann. Intern. Med.* 1993, **118**:681–688.

98. Richman DD, Bozzette SA: **The impact of the syncytium-inducing phenotype of human immunodeficiency virus on disease progression**. *J. Infect. Dis.* 1994, **169**:968–974.

99. Schuitemaker H: **Macrophage-tropic HIV-1 variants: initiators of infection and AIDS pathogenesis?** 1994 *Journal of Leukocyte Biology* vol. 56 no. 3 218-224.

100. Casper CH, Clevestig P, Carlenor E, Leitner T, Anzen B: **Link between the X4 phenotype in human immunodeficiency virus type 1 infected mothers and their children, despite the early presence of R5 in the child.** *J Infect Dis* 2002, **186**:914-921.

101. Davenport MP, Zaunders JJ, Hazenburg MD, Schuitemaker H, van Rij RP. **Cell turnover and cell tropism in HIV-1 infection.** *Trends Microbiol* 2002 **10**:275-278.

102. Harouse JM, Buckner C, Gettie A, Fuller R, Bohm R, Blanchard J, Cheng-Mayer C: **CD8 T cell-mediated CXC chemokine receptor 4-simian/human immunodeficiency virus suppression in dually infected rhesus macaques**. Proc Natl Acad Sci U S A. 2003, **100**(19):10977-82.

103. Cornelissen M, Mulder-Kampinga G, Veenstra J, Zorgdrager F, Kuiken C, Hartman S, Dekker J, van der Hoek L, Sol C, Coutinho R et al. **Sycytium-inducing (SI) phenotype suppression at seroconversion after intramuscular inoculation of a non-syncytium-inducing/SI phenotypically mixed human immunodeficiency virus population**. *J Virol.* 1995, (**3**):1810-8.

104. Callaway DS, Ribeiro RM, Nowak MA. **Virus phenotype switching and disease progression in HIV-1 infection.** *Proc. R. Soc*. *Lond B*. 1999, **266**:2523-2530.

105. Schutten M, van Baalen CA, Guillon C, Huisman RC, Boers PH, Sintnicolaas K, Gruters RA, Osterhaus AD: **Macrophage Tropism of Human Immunodeficiency Virus Type 1 Facilitates In Vivo Escape from Cytotoxic T-Lymphocyte Pressure**. *J Virol.* 2001, (**6**):2706-9.

106. Lee B, Sharron M, Montaner LJ, Weissman D, Doms RW: **Quantification of CD4, CCR5, and CXCR4 levels on lymphocyte subsets, dendritic cells, and differentially conditioned monocyte-derived macrophages.** *Proc Natl. Acad Sci. U.S.A* 1999, **96**:5215-5220.

107. Blaak H, van't Wout AB, Brouwer M, Hooibrink B, Hovenkamp E, Schuitemaker H: **In vivo HIV-1 infection of DC45RA(+)CD4(+) T cells is established primarily by syncytium-inducing variants and correlates with the rate of CD4(+) T cell decline.** *Proc.Natl. Acad Sci. U.S.A* 2000, **97**:1269-1274.

108. Van Ril RP, Blaak H, Visser JA, Brouwer M, Rientsma R, Broersen S, de Roda Husman AM, Schuitemaker H: **Differential coreceptor expression allows for independent evolution of non-syncytium-inducing and syncytium-inducing HIV-1**. *J Clin. Invest.* 2000, **106**: 1039-1052.

109. Veazey R. Lackner A: **The mucosal immune system and HIV-1 infection.** *AIDS Rev*. 2004, **5**:245-252.

110. Hazenburg MD, Stuart JW, Otto SA, Borleffs JC, Boucher CA, de Boer RJ, Miedema F, Hamann D: **T –cell division in himan immunodeficiency cirus (HIV)-1 infection is mainly sue to immune activation: a longitudinal analysis in patients before and during highly active antiretroviral therapy (HAART).** *Blood* 2000, **95**:249-255.

111. Ribeiro RM, Hazenberg MD, Perelson AS, Davenport MP: **Naive and memory cell turnover as drivers of CCR5-to-CXCR4 tropism switch in Human Immunodeficiency Virus Type 1: implications for therapy.** *J Virol* 2006, **80**: 802-809.

112. Weinberger AD, Perelson AS: **Persistance and emergence of X4 virus in HIV infection.** *Math Biocsi Eng.* 2011, **8**(2):605-626.

113. Coetzer M, Nedellec R, Salkowitz J, McLaughlin S, Liu Y, Heath L, Mullins JI, Mosier DE: **Evolution of CCR5 Use before and during Coreceptor Switching** *Virology*, 2006, **356**:95–105.

114. Rinaldo CR, Gupta P, Huang XL, Fan Z, Mullins JI, Gange S, Farzadegan H, Shankarappa R, Munoz A, Margolick JB: **Anti-HIV type 1 memory cytotoxic T lymphocyte responses associated with changes in CD4+ T cell numbers in progression of HIV type 1 infection.** *AIDS Res. Hum. Retrovir*. 1998, **14**:1423-1433.

115. Perelson AS, Nelson PW: **Mathematical Analysis of HIV-1 Dynamics in Vivo** *Society for Industrial and Applied Mathematics* 1999 **41**(1)3–44.

116. Tasca S, Siu-Hong Ho, Cheng-Mayer C: **R5X4 Viruses Are Evolutionary, Functional, and Antigenic Intermediates in the Pathway of a Simian-Human Immunodeficiency Virus Coreceptor Switch**. *J. Virol.* 2008, **82**:(14)7089-7099

117. Sacha JB, Chung C, Rakasz EG, Spencer SP, Jonas AK, Bean AT, Lee W, Burwitz BJ, Stephany JJ, Loffredo JT, Allison DB, Adnan S, Hoji A, Wilson NA, Friedrich TC, Lifson JD, Yang OO, Watkins DI: **Gag-specific CD8$^+$ T lymphocytes recognize infected cells before AIDS-virus integration and viral protein expression**. *J Immunol* 2007, **178**:2746-2754.

118. Buseyne F, Le Gall S, Boccaccio C, Abastado JP, Lifson JD, Arthur LO, Riviere Y, Heard JM, Schwartz O: **MHC-I-restricted presentation of HIV-1 virion antigens without viral replication**. *Nat Med* 2001, **7**:344-349.

119. Kloverpris HN, Payne RP, Sacha JB, Rasaiyaah JT, Chen F, Takiguchi M, Yang OO, Towers GJ, Goulder P, Prado JG: **Early antigen presentation of protective HIV-1 KF11Gag and KK10Gag epitopes from incoming viral particles facilitates rapid recognition of infected cells by specific CD8$^+$ T cells**. *J Virol* 2013, **87**:2628-2638.

120. Graf EH, Pace MJ, Peterson B, Lynch LJ, Chukwulebe SB, Mexas AM, Shaheen F, Martin JN, Deeks SG, Connors M, Migueles S, O'Doherty U: **Gag-positive reservoir cells are susceptible to HIV-specific cytotoxic T lymphocyte mediated clearance**. *PLoS One* 2013, 8:e71879.

121. Buckheit RW III, Siliciano RF, Blankson JN: **Primary CD8$^+$ T cells from elite suppressors effectively eliminate non-productively HIV-1 infected resting and activated CD4+ T cells**. *Retrovirology* 2013, **10**:68.

122. Zhang H, Zhou Y, Alcock C, Kiefer T, Monie D, Siliciano J, Li Q, Pham P, Cofrancesco J, Persaud D, Siliciano RF: **Novel single-cell–level phenotypic assay**

for residual drug susceptibility and reduced replication capacity of drug-resistant human immunodeficiency virus type 1. *J. Virol*. 2004, **78**:1718-1729.

123. Kellam P, Larder BA: **Recombinant virus assay: a rapid, phenotypic assay for assessment of drug susceptibility of human immunodeficiency virus type 1 isolates.** *Antimicrob Agents Chemother*. 1994, **38**:23-30.

124. O'Doherty U, Swiggard WJ, Malim MH: **Human immunodeficiency virus type 1 spinoculation enhances infection through virus budding**. *J Virol* 2000, **74**(21):10074-10080.

125. Saez-Cirion A, Sinet M, Shin SY, Urrutia A, Versmisse P, Lacabaratz C, Boufassa F, Avettand-Fenoel V, Rouzioux C, Delfraissy JF, Barre-Sinoussi F, Lambotte O, Venet A, Pancino G: **ANRS EP36 HIV Controllers Study Group:** Heterogeneity in HIV suppression by CD8 T cells from HIV controllers: association with Gag-specific CD8 T cell responses. *J Immunol* 2009, **182**(12):7828-7837.

126. Saez-Cirion A, Lacabaratz C, Lambotte O, Versmisse P, Urrutia A, Boufassa F, Barre-Sinoussi F, Delfraissy JF, Sinet M, Pancino G, Venet A: **EP36 HIV Controllers Study Group**: **HIV controllers exhibit potent CD8 T cell capacity to suppress HIV infection ex vivo and peculiar cytotoxic T lymphocyte activation phenotype**. *Proc Natl Acad Sci USA* 2007, **104**(16):6776-6781.

127. Pohlmeyer CW. Buckheit RW III, Siliciano RF, Blankson JN: **$CD8^+$ T cells from HLA-B*57 elite suppressors effectively suppress replication of HIV-1 escape mutants.** *Retrovirology* 2013, **10**:152

Curriculum Vitae
Melissa Zarr

CURRENT POSITION: Graduate Student with Dr. Robert Siliciano, Johns Hopkins University School of Medicine, Department of Pharmacology and Molecular Sciences, Baltimore MD

PERSONAL INFORMATION:

Address: 105 N Ann st
Baltimore MD 21231
Phone: 480-242-8108
Email: melissazarr@gmail.com

EDUCATION:

2000-2004	Mountain View High School, Mesa AZ
2004-2008	Reed College, Portland OR
2008-2014	Johns Hopkins University School of Medicine

PUBLICATIONS:

Peer- Reviewed Articles:

1. **Zarr** MA, Siliciano RF. Stoichiometric Parameters of HIV-1 Entry. Under Review

2. Avery LB, **Zarr** MA, Bakshi RP, Siliciano RF, Hendrix CW. Increasing Extracellular Protein Concentration Reduces Intracellular Antiretroviral Drug Concentration and Antiviral Effect. AIDS Res Hum Retroviruses. 2013 May 22.

3. Jilek BL, **Zarr** M, Sampah ME, Rabi SA, Bullen CK, Lai J, Shen L, Siliciano RF. A quantitative basis for antiretroviral therapy for HIV-1 infection. Nat Med. 2012 Feb 19;18(3):446-51. doi: 10.1038/nm.2649.

4. Mellies JL, Larabee FJ, **Zarr** MA, Horback KL, Lorenzen E, Mavor D. Ler interdomain linker is essential for anti-silencing activity in enteropathogenic Escherichia coli. Microbiology. 2008 Dec;154(Pt 12):3624-38. doi: 10.1099/mic.0.2008/023382-0.

Abstracts:

Zarr MA, Siliciano RF. "Tropism Specific Stoichiometric Parameters of HIV-1 Entry" Poster at the 20th Conference on Retroviruses and Opportunistic Infections [CROI], Atlanta GA, March 2013

REFERENCES:

Robert F. Siliciano M.D., Ph.D.
733 N. Broadway, 879 MRB
Baltimore, MD 21205
Phone: 410-955-2958
E-mail: rsiliciano@jhmi.edu
Graduate research mentor

Joel N. Blankson M.D., Ph.D.
733 N. Broadway, 871 MRB
Baltimore, Md. 21205
Phone: 410-955-7757
E-mail: jblanks@jhmi.edu
Thesis committee member, Professor who shares lab space with Dr. Siliciano

L. Mario Amzel
725 N. Wolfe St., 606 WBSB
Baltimore, MD 21205
Phone: 410-955-3955
E-mail: mamzel@jhmi.edu
Assistant: Tammy Watson-
twatso13@jhmi.edu
Thesis committee member, Member of graduate board orals, Rotation project mentor
He can overlook e-mails so it is best to also contact his assistant Tammy